

Interpretable Deep Regression Models with Interval-Censored Failure Time Data

Changhui Yuan

School of Mathematics, Jilin University

and

Shishun Zhao

School of Mathematics, Jilin University

and

Shuwei Li

School of Economics and Statistics, Guangzhou University

and

Xinyuan Song

Department of Statistics, Chinese University of Hong Kong

and

Zhao Chen

School of Data Science, Fudan University

Abstract

Deep neural networks (DNNs) have become powerful tools for modeling complex data structures through sequentially integrating simple functions in each hidden layer. In survival analysis, recent advances of DNNs primarily focus on enhancing model capabilities, especially in exploring nonlinear covariate effects under right censoring. However, deep learning methods for interval-censored data, where the unobservable failure time is only known to lie in an interval, remain underexplored and limited to specific data type or model. This work proposes a general regression framework for interval-censored data with a broad class of partially linear transformation models, where key covariate effects are modeled parametrically while nonlinear effects of nuisance multi-modal covariates are approximated via DNNs, balancing interpretability and flexibility. We employ sieve maximum likelihood estimation by leveraging monotone splines to approximate the cumulative baseline hazard function. To ensure reliable and tractable estimation, we develop an EM algorithm incorporating stochastic gradient descent. We establish the asymptotic properties of parameter estimators and show that the DNN estimator achieves minimax-optimal convergence. Extensive simulations demonstrate superior estimation and prediction accuracy over state-of-the-art methods. Applying our method to the Alzheimer's Disease Neuroimaging Initiative dataset yields novel insights and improved predictive performance compared to traditional approaches.

Keywords: EM algorithm, Interval censoring, Partially linear model, Splines, Neural networks.

1 Introduction

In recent decades, neural networks have exhibited remarkable success in various fields, including medical image analysis (Sun et al., 2024), natural language processing (Devlin et al., 2019), and object detection (Ren et al., 2017). A typical neural network consists of an input layer, one or more hidden layers, and an output layer. By leveraging an activation function, operation at each neuron is a nonlinear transformation for the simple weighted sum of the previous layer’s outputs. Neural networks have been theoretically recognized as a remarkable tool to approximate unknown functions. For example, Cybenko (1989) and Hornik et al. (1989) showed that shallow neural networks can approximate any continuous function with any degree of accuracy, even with a single hidden layer. A deep neural network (DNN) with multiple hidden layers and few nodes per layer can attain better representational capability than a shallow neural network with fewer than exponentially many nodes, which is an appealing advantage of DNN (Telgarsky, 2015).

In survival analysis, neural networks have spawned vast variants of the classical Kaplan-Meier estimator and regression models. To name a few, Katzman et al. (2018) modeled the complex interactions between covariates and therapies with a DNN in personalized treatment recommendations. Ren et al. (2019) investigated more flexible DNN-based Kaplan-Meier estimators. Kvamme et al. (2019) developed time-to-event prediction methods by adopting the neural network versions of the proportional hazards (PH) model. Tong and Zhao (2022) proposed a nuclear-norm-based imputation method, extending the work of Katzman et al. (2018) to handle missing covariates.

Recently, motivated by DNN’s powerful approximation ability, nonparametric and partially linear regression models have revived in survival analysis (Xie and Yu , 2021; Zhong et al., 2022; Sun and Ding, 2023; Wu et al., 2024). In particular, partially linear models

attract much attention since they can flexibly model linear and nonlinear covariate effects on the failure event of interest (Fan et al., 1997; Huang, 1999; Chen and Jin, 2006; Lu and Zhang, 2010; Lu and McMahan, 2018). Traditional estimation methods generally focus on constructing kernel-based estimating equations or using sieves, such as splines and local polynomials, to approximate the nonlinear component of the model. When the dimension of nonlinear covariates is large, the methods above suffer from the curse of dimensionality, which hinders their practical utility. In contrast, as shown by Schmidt-Hieber (2020) and Bauer and Kohler (2019), DNN can remedy the curse of dimensionality that often appears in nonparametric regressions, and the resulting estimators can achieve the optimal minimax convergence rate. For traditional right-censored data, Zhong et al. (2022) provided a partially linear PH model with DNN representing the nonlinear function of covariates, circumventing the curse of dimensionality and rendering a clear interpretation of interested covariate effects on a survival endpoint.

Interval-censored failure time data mean that the failure time of interest (e.g., the onset time of an asymptomatic disease) cannot be observed precisely and is only known to lie in a time interval formed by periodic examinations or cross-sectional screening. This type of censored data is ubiquitous in scientific studies, including but not limited to clinical trials, epidemiological surveys and sociological investigations. A simple type of interval-censored data investigated extensively is called current status data, where each failure time is either larger or smaller than one observation time (Sun, 2006). The analysis of interval-censored data is essential, and many studies have emerged (Huang, 1996; Zhang et al., 2010; Lu and McMahan, 2018; Lee et al., 2022; Li and Peng, 2023; Yuan et al., 2024). For example, Wang et al. (2016) and Zeng et al. (2016) proposed maximum likelihood estimation procedures for semiparametric PH and transformation models. Despite a rich literature on interval-

censored data, exploring DNN’s utility in partially linear models is relatively limited. The only available methods were Wu et al. (2024) and Du et al. (2024), which concerned sieve maximum likelihood analysis of current status and interval-censored data, respectively. It is worth pointing out that the two aforementioned methods were built upon the simple PH model, in which the PH assumption may be fragile, especially in long-term studies involving chronic diseases (Zeng and Lin, 2006).

Exploring DNN-based models and associated reliable estimation procedures is essential to offering a highly flexible regression framework for analyzing interval-censored data. Besides enhancing the model capability and prediction accuracy, such an exploration can render reliable inferences by positing weak model assumptions. The present study investigates this critical problem through a general DNN-based partially linear transformation model. It encompasses the popular partially linear PH and proportional odds (PO) models as specific cases and is highly explanatory while maintaining sufficient flexibility. We employ monotone splines and DNN to approximate the cumulative baseline hazard function and other nonparametric components. We resort to sieve maximum likelihood estimation and develop an expectation-maximization (EM) algorithm with stochastic gradient descent (SGD) optimization embedded in the maximization step. The proposed algorithm is robust to initialization, which substantially relieves the burden of parameter tuning in training the DNN-based model, and yields the sieve estimators in a reliable and tractable way. Under certain smoothness and structure assumptions commonly used in the analysis of nonparametric models, the asymptotic properties of our proposed estimator are established. In particular, the DNN-based estimator is shown to achieve the minimax optimal convergence. These properties ensure that the model is well-behaved and the estimator is consistent and efficient, providing a solid theoretical foundation for our approach.

2 Methods

2.1 Model, Data Structure and Likelihood

Let \mathbf{X} be a p -dimensional covariate vector whose effect is of primary interest (e.g., treatment variables). Denote by \mathbf{W} a vector consisting of d nuisance covariates. Conditional on \mathbf{X} and \mathbf{W} , we posit that the failure time of interest T follows a partially linear transformation model, where the conditional cumulative hazard function of T takes the form

$$\Lambda(t | \mathbf{X}, \mathbf{W}) = G [\Lambda(t) \exp\{\boldsymbol{\beta}^\top \mathbf{X} + \phi(\mathbf{W})\}]. \quad (1)$$

In model (1), $\Lambda(t)$ represents an unspecified cumulative baseline hazard function, $\boldsymbol{\beta}$ is a p -dimensional vector of regression parameters, $\phi(\mathbf{W})$ is an unknown smooth function that maps \mathbb{R}^d to \mathbb{R} , and $G(\cdot)$ is a prespecified increasing transformation function with $G(0) = 0$. Model (1) is general and includes various popular partially linear models as specific instances. For example, model (1) corresponds to the partially linear PH and PO models when setting $G(x) = x$ and $G(x) = \log(1 + x)$, respectively. In practical applications, it is common to consider the logarithmic transformation family, $G(x) = \log(1 + rx)/r$ ($r \geq 0$), in which $r = 0$ means $G(x) = x$. In fact, this class of transformation functions can be derived from the Laplace transformation as follows $G(x) = -\log \int_0^\infty \exp(-x\eta) f(\eta | r) d\eta$, where $f(\eta | r)$ is the density function of a gamma-distributed frailty variable with mean 1 and variance r (Kosorok et al., 2004). Since any constant in $\phi(\cdot)$ can be absorbed into $\Lambda(\cdot)$, we assume that $E\{\phi(\mathbf{W})\} = 0$, a frequently used condition as in Zhong et al. (2022) and others, to ensure an identifiable model.

Notably, traditional partially linear models, such as the partially linear additive PH and transformation models in Huang (1999) and Yuan et al. (2024), typically assume an additive form, $\sum_{j=1}^d \phi_j(W_j)$, for $\phi(\mathbf{W})$, where W_j is the j th component of \mathbf{W} , ϕ_j is an

unknown function with $j = 1, \dots, d$. Unlike the additive modeling described above, the proposed model (1) leaves the form of $\phi(\mathbf{W})$ completely unspecified and can accommodate multi-modal \mathbf{W} , thereby offering high flexibility. Furthermore, it is easy to see that model (1) can be equivalently expressed as

$$\log \Lambda(t) = -\boldsymbol{\beta}^\top \mathbf{X} - \phi(\mathbf{W}) + \epsilon,$$

where the error term ϵ has a distribution function $1 - \exp[-G\{\exp(x)\}]$. Therefore, $\boldsymbol{\beta}$ essentially represents the effect of \mathbf{X} on the transformed T .

We consider general interval-censored failure time data, where the exact failure time of interest T cannot be obtained but is only known to lie in a specific interval. More specifically, let $(L, R]$ be the interval that brackets T with $L < R$. Clearly, T is left censored if $L = 0$ and right censored when $R = \infty$. Define $\delta_L = 1$ if T is left censored, $\delta_R = 1$ when T is right censored, and $\delta_I = 1$ when T is strictly interval-censored (i.e., $L > 0$ and $R < \infty$). Then, the observed interval-censored data consist of n i.i.d. realizations of $\{L, R, \delta_L, \delta_I, \delta_R, \mathbf{X}, \mathbf{W}\}$, denoted by $\mathbf{O} = \{L_i, R_i, \delta_{L,i}, \delta_{I,i}, \delta_{R,i}, \mathbf{X}_i, \mathbf{W}_i; i = 1, \dots, n\}$. Notably, $\delta_{L,i} + \delta_{I,i} + \delta_{R,i} = 1$ for each individual i .

Under the conditional independence assumption between T_i and (L_i, R_i) given \mathbf{X}_i and \mathbf{W}_i , the observed data likelihood is given by

$$\begin{aligned} \mathcal{L}_{obs}(\boldsymbol{\beta}, \Lambda, \phi) &= \prod_{i=1}^n F(R_i | \mathbf{X}_i, \mathbf{W}_i)^{\delta_{L,i}} \{F(R_i | \mathbf{X}_i, \mathbf{W}_i) - F(L_i | \mathbf{X}_i, \mathbf{W}_i)\}^{\delta_{I,i}} \{1 - F(L_i | \mathbf{X}_i, \mathbf{W}_i)\}^{\delta_{R,i}}, \end{aligned} \quad (2)$$

where $F(t | \mathbf{X}_i, \mathbf{W}_i) = 1 - \exp(-G[\Lambda(t) \exp\{\boldsymbol{\beta}^\top \mathbf{X}_i + \phi(\mathbf{W}_i)\}])$ is the distribution function of T_i given \mathbf{X}_i and \mathbf{W}_i .

Note that the likelihood (2) involves two infinite-dimensional functions $\Lambda(t)$ and $\phi(\mathbf{W})$, which are usually treated as nuisance functions in model (1). Since $\Lambda(t)$ is increasing

and satisfies $\Lambda(0) = 0$, it is routine to adopt a sieve approach, which approximates $\Lambda(t)$ by some surrogate function with a finite number of parameters. Herein, we consider employing monotone splines (Ramsay, 1988), rendering the following approximation:

$$\Lambda(\cdot) \approx \Lambda_{\boldsymbol{\gamma}}(\cdot) = \sum_{l=1}^{L_n} \gamma_l M_l(\cdot),$$

where γ_l 's are the nonnegative spline coefficients that ensure the monotonicity of $\Lambda_{\boldsymbol{\gamma}}(\cdot)$, $M_l(\cdot)$'s represent the integrated spline basis functions, each of which is nondecreasing from 0 to 1, and $\boldsymbol{\gamma} = (\gamma_1, \dots, \gamma_{L_n})^\top$. In order to use monotone splines, one needs to specify the degree denoted by d_M and an interior knot set specified within a time range. In particular, the overall smoothness of the basis functions is determined by the degree. For instance, monotone splines with degrees of 1, 2, or 3 correspond to linear, quadratic, or cubic splines, respectively. More dense interior knots in a time range offer more flexible modeling in that range. In practical applications, the interior knots can be set to be an equally spaced grid of points between the minimum and maximum observation times or quantiles of the observation times. After specifying the degree and interior knots, one can determine $L_n = p_n + d_M$ spline basis functions, where p_n is the interior knot number.

2.2 Deep Neural Network

To estimate $\phi(\mathbf{W})$, traditional methods, such as kernel smoothing, generally suffer from the curse of dimensionality especially when encountering a large-dimensional \mathbf{W} . To circumvent this obstacle, we herein consider approximating $\phi(\mathbf{W})$ with the powerful DNN denoted by $\phi_{\boldsymbol{\alpha}}(\mathbf{W})$, where $\boldsymbol{\alpha}$ is a vector consisting of all unknown parameters in the DNN. Let q be a positive integer representing the number of hidden layers in the DNN. A typical $(q + 1)$ -layer DNN consists of an input layer, q hidden layers, and an output layer. Denote by $\mathbf{h} = (h_0, h_1, \dots, h_q, h_{q+1})$ some positive integer sequence, where h_0 is the dimension of

input variables in the input layer, h_j is the number of neurons for the j th hidden layer with $j = 1, \dots, q$, and h_{q+1} is the dimension of the output layer. A $(q + 1)$ -layer DNN with layer-width \mathbf{h} is essentially a composite function $\phi_{\boldsymbol{\alpha}}: \mathbb{R}^{h_0} \rightarrow \mathbb{R}^{h_{q+1}}$ recursively defined as

$$\begin{aligned}
\phi_{\boldsymbol{\alpha}}(\mathbf{x}) &= \boldsymbol{\omega}_q \phi_q(\mathbf{x}) + \mathbf{v}_q, \\
\phi_q(\mathbf{x}) &= \sigma(\boldsymbol{\omega}_{q-1} \phi_{q-1}(\mathbf{x}) + \mathbf{v}_{q-1}), \\
&\vdots \\
\phi_2(\mathbf{x}) &= \sigma(\boldsymbol{\omega}_1 \phi_1(\mathbf{x}) + \mathbf{v}_1), \\
\phi_1(\mathbf{x}) &= \sigma(\boldsymbol{\omega}_0 \mathbf{x} + \mathbf{v}_0),
\end{aligned} \tag{3}$$

where $\boldsymbol{\omega}_0, \dots, \boldsymbol{\omega}_q$ are the unknown weight matrices, and $\mathbf{v}_0, \dots, \mathbf{v}_q$ are the unknown vectors including the shift term (i.e., intercept). For each $j = 0, 1, \dots, q$, $(\boldsymbol{\omega}_j)_{s,k}$, the (s, k) th entry of $\boldsymbol{\omega}_j$, denotes the weight associated with the k th neuron in layer j to the s th neuron in layer $j + 1$, and the vector entry $(\mathbf{v}_j)_s$ represents a shift term associated with the s th neuron in layer $j + 1$. The activation functions denoted by σ perform component-wise nonlinear transformations on vectors as $\sigma((x_1, \dots, x_{h_j})^\top) = (\sigma(x_1), \dots, \sigma(x_{h_j}))^\top$ for $j = 1, \dots, q$. Thus, for each $j = 1, \dots, q$, $\phi_j = (\phi_{j1}, \dots, \phi_{jh_j})^\top$ maps $\mathbb{R}^{h_{j-1}}$ to \mathbb{R}^{h_j} . For illustration, Figure 1 presents the network structure of a 4-layer DNN with $\mathbf{h} = (h_0, h_1, h_2, h_3, h_4) = (4, 3, 3, 2, 1)$.

Some commonly adopted activation functions in deep learning include sigmoid, tanh, rectified linear unit (ReLU), and their variants (He et al., 2015; Chen et al., 2020). In our DNN architecture, the Scaled Exponential Linear Unit (SeLU) (Klambauer et al., 2017) is the activation function. The SeLU activation function can be considered a variant of the simple ReLU and has several advantages over ReLU. For example, unlike ReLU, which outputs zero for negative inputs, SeLU has a non-zero output in the negative region, keeping potentially important neurons active in the whole network architecture (Dubey et

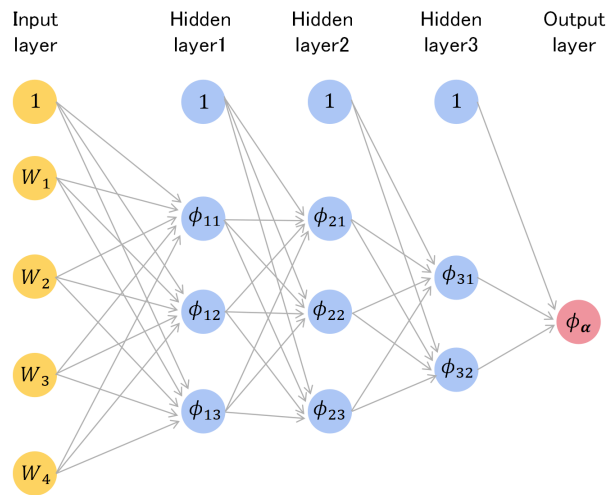


Figure 1: The network structure of a 4-layer DNN with $\mathbf{h} = (h_0, h_1, h_2, h_3, h_4) = (4, 3, 3, 2, 1)$. The filled circle over the neurons of the input layer or each hidden layer implies the existence of a shift term.

al., 2022). Therefore, adopting the SeLU activation function can lead to stable and efficient training of DNN.

Note that, in a DNN, if neurons in any two adjacent layers are fully connected, the dimension of $\boldsymbol{\alpha}$ would be large, which may lead to overfitting. In practical implementations, pruning weights such that the network’s layers are only sparsely connected is a routine to relieve overfitting (Silver et al., 2017; Schmidt-Hieber, 2020). Specifically, define a class of sparse neural networks as

$$\mathcal{F}(s, q, \mathbf{h}, B) = \left\{ \phi_{\boldsymbol{\alpha}} : \phi_{\boldsymbol{\alpha}} \text{ is a DNN with } (q + 1) \text{ layers and width vector } \mathbf{h} \text{ such that} \right.$$

$$\left. \begin{aligned} \max\{\|\boldsymbol{\omega}_j\|_{\infty}, \|\mathbf{v}_j\|_{\infty}\} &\leq 1 \text{ for } j = 0, \dots, q, \\ \sum_{j=0}^q (\|\boldsymbol{\omega}_j\|_0 + \|\mathbf{v}_j\|_0) &\leq s, \|\phi_{\boldsymbol{\alpha}}\|_{\infty} \leq B \end{aligned} \right\},$$

where $s \in \mathbb{R}_+$, the set of all positive real numbers, $B > 0$, $\|\cdot\|_{\infty}$ denotes the sup-norm of a matrix, vector, or function, and $\|\cdot\|_0$ is the number of nonzero entries of a matrix or vector. The sup-norm of a function ϕ is defined as $\|\phi\|_{\infty} = \sup_{\mathbf{W} \in \mathbb{R}^d} |\phi(\mathbf{W})|$. Typically, the sizes of the learned matrices $\boldsymbol{\omega}_j$ ’s and vectors \mathbf{v}_j ’s are not large, especially when the initial matrices and vectors used for starting the SGD training are relatively small. Thus, as in Schmidt-Hieber (2020) and others, we assume that the unknown parameters in the DNN are bounded by one. In a DNN, the parameter s governs the network sparsity, and its selection typically leverages the dropout technique within each hidden layer, which randomly ignores partial neurons based on a specified dropout rate (Srivastava et al., 2014). This strategy enhances model robustness by preventing over-reliance on particular neurons during training (Sun et al., 2024). In model (1), by approximating $\phi(\mathbf{W})$ with a DNN $\phi_{\boldsymbol{\alpha}} \in \mathcal{F} = \mathcal{F}(s, q, \mathbf{h}, \infty)$, where $h_0 = d$ and $h_{q+1} = 1$, we have the proposed deep partially linear transformation model.

2.3 Parameter Estimation

Based on the aforementioned spline and DNN approximations, the likelihood (2) can be rewritten as

$$\begin{aligned} \mathcal{L}_{obs}(\boldsymbol{\beta}, \boldsymbol{\gamma}, \boldsymbol{\alpha}) &= \prod_{i=1}^n F_n(R_i | \mathbf{X}_i, \mathbf{W}_i)^{\delta_{L,i}} \{F_n(R_i | \mathbf{X}_i, \mathbf{W}_i) - F_n(L_i | \mathbf{X}_i, \mathbf{W}_i)\}^{\delta_{I,i}} \{1 - F_n(L_i | \mathbf{X}_i, \mathbf{W}_i)\}^{\delta_{R,i}}, \end{aligned} \quad (4)$$

where $F_n(t | \mathbf{X}_i, \mathbf{W}_i) = 1 - \exp(-G[\Lambda_{\boldsymbol{\gamma}}(t) \exp\{\boldsymbol{\beta}^\top \mathbf{X}_i + \phi_{\boldsymbol{\alpha}}(\mathbf{W}_i)\}])$.

By the maximum likelihood principle, the estimator of $(\boldsymbol{\beta}, \boldsymbol{\gamma}, \boldsymbol{\alpha})$ denoted by $(\hat{\boldsymbol{\beta}}, \hat{\boldsymbol{\gamma}}, \hat{\boldsymbol{\alpha}})$ is defined as

$$(\hat{\boldsymbol{\beta}}, \hat{\boldsymbol{\gamma}}, \hat{\boldsymbol{\alpha}}) = \arg \max_{\boldsymbol{\beta} \in \mathbb{R}^p, \boldsymbol{\gamma} \in \mathbb{R}_+^{L_n}, \phi_{\boldsymbol{\alpha}} \in \mathcal{F}} \mathcal{L}_{obs}(\boldsymbol{\beta}, \boldsymbol{\gamma}, \boldsymbol{\alpha}).$$

Typically, from the computational aspect, performing direct maximization of likelihood (4) with some existing optimization functions in the statistical software is quite challenging due to the intractable form of (4) and many unknown parameters. The complexity is further magnified by including a neural network estimation. Such an optimization is not a simple task, even without the DNN $\phi_{\boldsymbol{\alpha}}(\cdot)$ under a simpler PH model (Wang et al., 2016).

To facilitate the estimation, we construct an EM algorithm coupled with a three-stage data augmentation and SGD to maximize (4) and obtain $(\hat{\boldsymbol{\beta}}, \hat{\boldsymbol{\gamma}}, \hat{\boldsymbol{\alpha}})$. Due to the space restriction, we defer the details of the proposed algorithm to Section S.1 of the supplementary materials. Empirically, the proposed algorithm has certain robustness to the choice of initial values, $\boldsymbol{\beta}^{(0)}$, $\boldsymbol{\gamma}^{(0)}$, and $\boldsymbol{\alpha}^{(0)}$. In practice, one can initialize the monotone spline coefficients with 0.01 and all regression coefficients with 0. We employ Keras’s default random initialization for all parameters in the DNN (Glorot and Bengio, 2010). Convergence of the algorithm is declared when the maximum absolute difference of the log-likelihood values between two successive iterations is less than a small positive threshold (e.g., 0.001).

3 Asymptotic Properties

We establish the asymptotic properties of our proposed estimators with the sieve estimation theory and empirical process techniques. Let $\hat{\boldsymbol{\theta}} = (\hat{\boldsymbol{\beta}}, \hat{\Lambda}, \hat{\phi})$ denote the proposed estimator of $\boldsymbol{\theta} = (\boldsymbol{\beta}, \Lambda, \phi)$, where $\hat{\boldsymbol{\beta}}$, $\hat{\Lambda}$, and $\hat{\phi}$ are the estimators of $\boldsymbol{\beta}$, Λ , and ϕ , respectively. Define $\boldsymbol{\theta}_0 = (\boldsymbol{\beta}_0, \Lambda_0, \phi_0)$, where $\boldsymbol{\beta}_0$, Λ_0 , and ϕ_0 represent the true values of $\boldsymbol{\beta}$, Λ , and ϕ , respectively. Let $\|\cdot\|$ and $\|\cdot\|_\infty$ denote the usual Euclidean norm and supremum norm, respectively. That is, for a vector $\boldsymbol{\beta} = (\beta_1, \dots, \beta_p)^\top$, $\|\boldsymbol{\beta}\| = (\sum_{i=1}^p \beta_i^2)^{1/2}$ and $\|\boldsymbol{\beta}\|_\infty = \max_i |\beta_i|$. For any matrix $\boldsymbol{\Sigma} = (\sigma_{ij})$, $\|\boldsymbol{\Sigma}\|_\infty = \max_{i,j} |\sigma_{ij}|$. The notation $X_n \lesssim Y_n$ indicates $X_n \leq MY_n$, $X_n \gtrsim Y_n$ indicates $X_n \geq MY_n$ for some constant $M > 0$. $X_n \asymp Y_n$ indicates $X_n \lesssim Y_n$ and $X_n \gtrsim Y_n$, which means that X_n is of the same order as Y_n . Define $X_n \wedge Y_n = \min\{X_n, Y_n\}$ and $X_n \vee Y_n = \max\{X_n, Y_n\}$. Let \mathbb{N}_+ denote the set of all positive integers and \mathbb{R}_+ represent the set of all positive real numbers. Define a Hölder class of smooth functions with $\xi_\phi > 0$, $S > 0$ and $\mathbb{D} \subset \mathbb{R}^d$ as

$$\Psi_d^{\xi_\phi}(\mathbb{D}, S) = \left\{ \phi : \mathbb{D} \rightarrow \mathbb{R} : \sum_{\boldsymbol{\nu} : |\boldsymbol{\nu}| < \xi_\phi} \|\partial^{\boldsymbol{\nu}} \phi\|_\infty + \sum_{\boldsymbol{\nu} : |\boldsymbol{\nu}| = \lfloor \xi_\phi \rfloor} \sup_{\mathbf{w}_1, \mathbf{w}_2 \in \mathbb{D}, \mathbf{w}_1 \neq \mathbf{w}_2} \frac{|\partial^{\boldsymbol{\nu}} \phi(\mathbf{w}_1) - \partial^{\boldsymbol{\nu}} \phi(\mathbf{w}_2)|}{\|\mathbf{w}_1 - \mathbf{w}_2\|_\infty^{\xi_\phi - \lfloor \xi_\phi \rfloor}} \leq S \right\},$$

where we use the multi-index notation $\partial^{\boldsymbol{\nu}} = \partial^{\nu_1} \dots \partial^{\nu_d}$ with $\boldsymbol{\nu} = (\nu_1, \dots, \nu_d)^\top \in \mathbb{N}_+^d$ and $|\boldsymbol{\nu}| = \sum_{j=1}^d \nu_j$, and $\lfloor \xi_\phi \rfloor$ is the largest integer that is strictly smaller than ξ_ϕ (Schmidt-Hieber, 2020).

Let $\tilde{k} \in \mathbb{N}_+$ and $\boldsymbol{\xi}_\phi = (\xi_{\phi_1}, \dots, \xi_{\phi_{\tilde{k}}})^\top \in \mathbb{R}_+^{\tilde{k}}$. Define $\bar{\boldsymbol{d}} = (\bar{d}_1, \dots, \bar{d}_{\tilde{k}+1})^\top \in \mathbb{N}_+^{\tilde{k}+1}$ and $\tilde{\boldsymbol{d}} = (\tilde{d}_1, \dots, \tilde{d}_{\tilde{k}})^\top \in \mathbb{N}_+^{\tilde{k}}$ with $\tilde{d}_j \leq \bar{d}_j$ for each $j = 1, \dots, \tilde{k}$. Let $\tilde{\xi}_{\phi i} = \xi_{\phi i} \prod_{j=i+1}^{\tilde{k}} (\xi_{\phi j} \wedge 1)$ for $i = 1, \dots, \tilde{k}$, and $\alpha_n = \max_{i=1, \dots, \tilde{k}} n^{-\tilde{\xi}_{\phi i} / (2\tilde{\xi}_{\phi i} + \bar{d}_i)}$. We further define a composite smoothness

function class, taking the form

$$\Psi(\tilde{k}, \boldsymbol{\xi}_\phi, \bar{\mathbf{d}}, \tilde{\mathbf{d}}, S) = \left\{ \phi = \varphi_{\tilde{k}} \circ \cdots \circ \varphi_1 : \varphi_i = (\varphi_{i1}, \dots, \varphi_{i\bar{d}_{i+1}})^\top \text{ and} \right. \quad (5)$$

$$\left. \begin{aligned} \varphi_{ij} &\in \Psi_{\tilde{d}_i}^{\xi_{\phi i}}([e_i, f_i]^{\tilde{d}_i}, S), \text{ for some } |e_i| \text{ and } |f_i| \leq S, i = 1, \dots, \tilde{k}, \\ j &= 1, \dots, \bar{d}_{i+1} \end{aligned} \right\},$$

where $S > 0$ and $\tilde{\mathbf{d}}$ represents the intrinsic dimension of a function. For instance, if $\mathbf{w} \in [0, 1]^{10}$,

$$\phi(\mathbf{w}) = \varphi_{31}(\varphi_{21}\{\varphi_{11}(w_1, w_2, w_3, w_4), \varphi_{12}(w_5, w_6)\}, \varphi_{22}\{\varphi_{13}(w_7), \varphi_{14}(w_8), \varphi_{15}(w_9, w_{10})\}),$$

and each φ_{ij} is twice continuously differentiable, then $\boldsymbol{\xi}_\phi = (2, 2, 2)$, $\tilde{k} = 3$, $\bar{\mathbf{d}} = (10, 5, 2, 1)$ and $\tilde{\mathbf{d}} = (4, 3, 2)$. Let $\ell^\infty[x, y]$ denote the space of bounded sequences on $[x, y]$. Define the function spaces $\bar{\Psi}_\Lambda = \{\Lambda \in \ell^\infty[a, b] : \Lambda \text{ is monotone increasing with } \Lambda(0) = 0 \text{ and } \Lambda(b) < \infty, \text{ where } [a, b] \text{ is the union support of } L \text{ and } R \text{ with } 0 \leq a < b < \infty\}$ and $\bar{\Psi}_\phi = \{\phi : \phi \in \Psi(\tilde{k}, \boldsymbol{\xi}_\phi, \bar{\mathbf{d}}, \tilde{\mathbf{d}}, S), E\{\phi(\mathbf{W})\} = 0\}$.

Let Θ be the product space defined as $\Theta = \mathcal{D} \times \bar{\Psi}_\Lambda \times \bar{\Psi}_\phi$, where \mathcal{D} is a compact subset of \mathbb{R}^p . For any $\boldsymbol{\theta}_1$ and $\boldsymbol{\theta}_2 \in \Theta$, define the distance $d(\boldsymbol{\theta}_1, \boldsymbol{\theta}_2)$ as

$$d(\boldsymbol{\theta}_1, \boldsymbol{\theta}_2) = (\|\boldsymbol{\beta}_1 - \boldsymbol{\beta}_2\|^2 + \|\Lambda_1 - \Lambda_2\|_{L_2}^2 + \|\phi_1 - \phi_2\|_{L_2}^2)^{1/2},$$

where $\|\cdot\|_{L_2}$ denotes the L_2 -norm over a specific interval. For instance, $\|\phi_1 - \phi_2\|_{L_2}^2 = \int_{\mathcal{W}} \{\phi_1(\mathbf{w}) - \phi_2(\mathbf{w})\}^2 dF_{\mathbf{W}}(\mathbf{w})$, where $F_{\mathbf{W}}(\mathbf{w})$ is the distribution function of \mathbf{W} , \mathcal{W} is the support of \mathbf{W} , $\phi_1 \in \bar{\Psi}_\phi$ and $\phi_2 \in \bar{\Psi}_\phi$.

Consider the set $\mathcal{T}_n = \{t_i\}_{i=1}^{p_n}$, where

$$a = t_0 < t_1 < \dots < t_{p_n} < t_{p_n+1} = b$$

forms a sequence of knots dividing the interval $[a, b]$ into $p_n + 1$ subintervals, and $p_n = O(n^\nu)$ with $0 < \nu < 0.5$. Define

$$\mathcal{M}(\mathcal{T}_n, d_M, B) = \left\{ \sum_{l=1}^{L_n} \gamma_l M_l(t) : 0 \leq \gamma_l \leq B \text{ for } l = 1, \dots, L_n, t \in [a, b] \right\},$$

where B is a large positive constant. To establish the asymptotic properties of $\hat{\boldsymbol{\theta}}$, we use the following regularity conditions.

- (C1) The true regression parameter vector $\boldsymbol{\beta}_0$ belongs to the interior of the compact set \mathcal{D} , $\Lambda_0 \in \bar{\Psi}_\Lambda$, the first derivative of Λ_0 is strictly positive and continuous on $[a, b]$, and $\phi_0 \in \bar{\Psi}_\phi$.
- (C2) The covariate vector $(\mathbf{X}^\top, \mathbf{W}^\top)^\top$ takes values in a bounded subset of \mathbb{R}^{p+d} , and its joint probability density function is bounded away from zero.
- (C3) For $\xi \geq 1$, the ξ th derivative of Λ_0 satisfies the Lipchitz condition on $[a, b]$. That is, there exists a constant c_Λ such that $|\Lambda_0^{(\xi)}(t_1) - \Lambda_0^{(\xi)}(t_2)| \leq c_\Lambda |t_1 - t_2|$, for any $t_1, t_2 \in [a, b]$.
- (C4) The maximum spacing between any two adjacent knots, $\Delta_\Lambda = \max_{1 \leq i \leq p_n+1} |t_i - t_{i-1}|$, is $O(n^{-\nu})$ with $0 < \nu < 0.5$. In addition, the ratio of the maximum and minimum spacings of the adjacent knots, $\Delta_\Lambda/\delta_\Lambda$, is uniformly bounded, where $\delta_\Lambda = \min_{1 \leq i \leq p_n+1} |t_i - t_{i-1}|$.
- (C5) For any $\boldsymbol{\beta} \neq \boldsymbol{\beta}_0$, $P(\boldsymbol{\beta}^\top \mathbf{X} \neq \boldsymbol{\beta}_0^\top \mathbf{X}) > 0$.
- (C6) In the DNN, $q = O(\log n)$, $s = O(n\alpha_n^2 \log n)$, and $n\alpha_n^2 \lesssim \min\{h_1, \dots, h_q\} \leq \max\{h_1, \dots, h_q\} \lesssim n$.
- (C7) For $\tilde{\xi} \geq 1$, the joint density $f(t, \mathbf{x}, \mathbf{w}, \delta_l, \delta_i, \delta_r)$ of $(T, \mathbf{X}, \mathbf{W}, \delta_L, \delta_I, \delta_R)$ with respect to t or \mathbf{w} has bounded $\tilde{\xi}$ th partial derivatives.

(C8) If $\boldsymbol{\beta}^\top \mathbf{X} + f(t) = 0$ for any $t \in [a, b]$ with probability one, then $\boldsymbol{\beta} = 0$ and $f(t) = 0$ for $t \in [a, b]$.

Conditions (C1) and (C2) impose boundedness on the true parameters and covariates, which are commonly employed in the literature of interval-censored data analysis (Huang, 1996; Zhang et al., 2010; Zeng et al., 2016). Condition (C3) pertains to the smoothness of $\Lambda_0(t)$, and Condition (C4) is frequently adopted to establish the convergence rate and asymptotic normality of a sieve estimator (Lu et al., 2007). Condition (C5) pertains to the model identification. Condition (C6) specifies a neural network's structure (e.g., the sparsity and layer-width) in $\mathcal{F}(s, q, \mathbf{h}, B)$ and serves as a balance between approximation error and estimation error (Zhong et al., 2022). Condition (C7) is used to show that the score operators for nonparametric components trend toward zero in the least favorable direction, facilitating the asymptotic normality of parametric component estimators. Condition (C8) holds if the matrix $E([1, X^\top]^\top [1, X^\top])$ is nonsingular. The asymptotic behaviors of $\hat{\boldsymbol{\theta}}$ are described in the following three theorems with the detailed proofs sketched in Section S.2 of the supplementary materials.

Theorem 1. *Suppose that conditions (C1)–(C5) hold, we have $\|\hat{\boldsymbol{\beta}} - \boldsymbol{\beta}_0\| \rightarrow 0$ and $\|\hat{\Lambda} - \Lambda_0\|_{L_2} + \|\hat{\phi} - \phi_0\|_{L_2} \rightarrow 0$, as $n \rightarrow \infty$.*

Theorem 2. *Suppose that conditions (C1)–(C6) hold and $1/(2\xi + 1) < \nu < 1/(2\xi)$ with $\xi \geq 1$, we have $d(\hat{\boldsymbol{\theta}}, \boldsymbol{\theta}_0) = O_p(\alpha_n \log^2 n + n^{-\xi\nu})$.*

Theorem 3. *Suppose that conditions (C1)–(C8) hold, then*

$$n^{1/2}(\hat{\boldsymbol{\beta}} - \boldsymbol{\beta}_0) \xrightarrow{d} \mathcal{N}\{0, \mathbf{I}^{-1}(\boldsymbol{\beta}_0)\}, \text{ as } n \rightarrow \infty,$$

where \xrightarrow{d} denotes the convergence in distribution and $\mathbf{I}(\boldsymbol{\beta}_0)$ is the information matrix of $\boldsymbol{\beta}_0$ defined in Section S.2 of the supplementary materials. In other words, the covariance

matrix of $n^{1/2}(\hat{\boldsymbol{\beta}} - \boldsymbol{\beta}_0)$ attains the semiparametric efficiency bound.

To make inference on regression vector of interest $\boldsymbol{\beta}_0$, one often needs to estimate the covariance matrix of $\hat{\boldsymbol{\beta}}$. Herein, we employ a simple numerical profile likelihood approach. Specifically, define $\mathcal{L}_i(\boldsymbol{\beta}, \Lambda, \phi)$ as the logarithm of the observed-data likelihood function for subject i in $\mathcal{L}_{obs}(\boldsymbol{\beta}, \Lambda, \phi)$ (2). For a fixed $\boldsymbol{\beta}$, define $(\hat{\Lambda}_{\boldsymbol{\beta}}, \hat{\phi}_{\boldsymbol{\beta}}) = \operatorname{argmax}_{\Lambda, \phi} \log \mathcal{L}_{obs}(\boldsymbol{\beta}, \Lambda, \phi)$, which can be obtained via the proposed EM algorithm by only updating $\boldsymbol{\gamma}$ and $\boldsymbol{\alpha}$. Thus, the covariance matrix of $\hat{\boldsymbol{\beta}}$ is given by $(n\hat{\mathbf{I}})^{-1}$, where

$$\hat{\mathbf{I}} = n^{-1} \sum_{i=1}^n \left\{ \left. \frac{\partial}{\partial \boldsymbol{\beta}} \mathcal{L}_i(\boldsymbol{\beta}, \hat{\Lambda}_{\boldsymbol{\beta}}, \hat{\phi}_{\boldsymbol{\beta}}) \right|_{\boldsymbol{\beta}=\hat{\boldsymbol{\beta}}} \right\}^{\otimes 2}.$$

In the above, $\mathbf{a}^{\otimes 2} = \mathbf{a}\mathbf{a}^{\top}$ for a column vector \mathbf{a} . For each i , to calculate $\left. \frac{\partial}{\partial \boldsymbol{\beta}} \mathcal{L}_i(\boldsymbol{\beta}, \hat{\Lambda}_{\boldsymbol{\beta}}, \hat{\phi}_{\boldsymbol{\beta}}) \right|_{\boldsymbol{\beta}=\hat{\boldsymbol{\beta}}}$, one can readily employ a first-order numerical difference method given by

$$\frac{pl_i(\hat{\boldsymbol{\beta}} + h_n \mathbf{e}_j) - pl_i(\hat{\boldsymbol{\beta}})}{h_n},$$

where \mathbf{e}_j is a p -dimensional vector with 1 at the j th position and 0 elsewhere, h_n is a constant with the same order as $n_t^{-1/2}$, n_t represents the sample size of the training data, and $pl_i(\boldsymbol{\beta}) = \mathcal{L}_i(\boldsymbol{\beta}, \hat{\Lambda}_{\boldsymbol{\beta}}, \hat{\phi}_{\boldsymbol{\beta}})$. Our numerical experiments suggest that this profile likelihood variance estimation method works well in finite samples.

4 Simulation Study

We conducted extensive simulations to assess the empirical performance of the proposed deep regression method in finite samples. Comparison results with the deep PH model (Du et al., 2024), the partially linear additive transformation model (Yuan et al., 2024), the penalized PH model with linear covariate effects (Zhao et al., 2020), and the transformation model with linear covariate effects (Zeng et al., 2016) were also included to demonstrate the

advantages of the proposed method. In model (1), we let $\mathbf{X} = (X_1, X_2)^\top$, where X_1 and X_2 were generated from the standard normal distribution and the Bernoulli distribution with a success probability of 0.5, respectively. The length of \mathbf{W} was set to $d = 4$ or 10, and each component of $\mathbf{W} = (W_1, \dots, W_d)^\top$ followed the uniform distribution on $(-1, 1)$. The failure time T was generated according to model (1), where $\boldsymbol{\beta} = (\beta_1, \beta_2)^\top = (0.5, -0.5)^\top$, $G(x) = x$ or $\log(1 + x)$, $\Lambda(t) = 0.1t$ if $d = 4$ and $\Lambda(t) = 0.2t$ if $d = 10$. Notably, model (1) reduces to the deep partially linear PH and PO models by specifying $G(x) = x$ and $G(x) = \log(1 + x)$, respectively. For the setting of $d = 4$, we investigated the following three cases for $\phi(\mathbf{W})$:

$$\text{Case 1: } \phi(\mathbf{W}) = W_1 + W_2/2 + W_3/3 + W_4/4,$$

$$\text{Case 2 : } \phi(\mathbf{W}) = W_1^2 + 2W_2^2 + W_3^3 + \sqrt{W_4 + 1} - 1.9, \text{ and}$$

$$\text{Case 3 : } \phi(\mathbf{W}) = W_1^2 + \log(W_2 + 2)/2 + 2\sqrt{W_3W_4 + 1} - 2.6.$$

For the setting of $d = 10$, the true $\phi(\mathbf{W})$ was specified as

$$\text{Case 4: } \phi(\mathbf{W}) = W_1 + W_2/2 + \dots + W_9/9 + W_{10}/10,$$

$$\text{Case 5 : } \phi(\mathbf{W}) = W_1 + W_2 + \dots + W_8 + W_9^2 + 2W_{10}^2 - 1, \text{ or}$$

$$\text{Case 6 : } \phi(\mathbf{W}) = \log(W_1 + 1) + W_2^2W_3^3 + W_4/2 + \sqrt{W_5W_6 + 1} + W_7^2 + \exp(W_8/2) + (W_9 + W_{10})^2 - 2.7.$$

Constants, -1.9, -2.6, -1.0, and -2.7, were included in $\phi(\mathbf{W})$ to ensure that $E\{\phi(\mathbf{W})\}$ is close to 0.

To create interval censoring, we generated a sequence of observation times, where the gap between any two consecutive observations followed an exponential distribution with a mean of 0.5. We set the study length to 8, after which no further observations happened. Then, the interval $(L, R]$ that contains T was determined by contrasting the generated T with the observation times. On average, the above configurations gave approximately 5%

to 16% left-censored observations and 34% to 61% right-censored ones.

To apply the proposed estimation method, we approximated $\Lambda(t)$ with cubic monotone splines, in which 3 interior knots were placed at the equally spaced quantiles within the minimum and maximum observation times. We set the sample size n to 500 or 1000 and used 200 replicates. For each simulation replicate, 16% of the simulated data were treated as the validation data used to tune hyperparameters, including the layer number, learning rate, and tuning parameter of the L_1 penalty used in the SGD algorithm. We then specified 64% of the simulated data as the training set utilized to estimate the unknown parameters based on the selected optimal hyperparameter configuration. Therefore, the actual sample sizes used to obtain the parameter estimation results were 320 and 640 for $n = 500$ and 1000, respectively. The remaining 20% of the data served as test data to evaluate the estimation performance for $\phi(\mathbf{W})$.

We considered 2 or 3 hidden layers, 50 neurons in each hidden layer, and SeLU activation function in building the neural network. To train the network, we set the tuning parameter in the L_1 penalty to 0.01 or 0.05 and the learning rate to 0.0001 or 0.0003. The mini-batch size in the SGD algorithm was set to 50. The neural network was trained for 20 epochs during each iteration of the proposed EM algorithm. We applied the dropout regularization with a rate of 0.1 to prevent overfitting and selected the optimal hyperparameter combination with the maximum likelihood principle on the validation data.

Table 1 summarizes the simulation results for the regression parameter estimates under the PH model ($G(x) = x$). Based on 200 replications, the used metrics include the estimation bias (Bias) calculated by the average of the estimates minus the true value, the sample standard error (SSE) of the estimates, the average of the standard error estimates (SEE), and the 95% coverage probability (CP95) formed by the normal approximation. Results

in Table 1 indicate that the proposed method gives sensible performance in finite samples. The biases of all regression parameter estimates are small, and the ratio of SSE to SEE is close to 1, suggesting that our profile-likelihood variance estimation approach performs adequately. All coverage probabilities are close to the nominal value, affirming the validity of using a normal approximation for the asymptotic distribution of regression parameter estimates. As anticipated, the proposed method’s estimation efficiency exhibited by SSEs and SEEs improves when the sample size increases from 500 to 1000.

To manifest the usefulness of the proposed deep regression method, we reanalyzed the above simulated data with four comparative state-of-the-art methods. They include the deep learning approach for the partially linear PH model abbreviated as “Deep PH” (Du et al., 2024), the sieve maximum likelihood estimation (MLE) approach for the partially linear additive transformation model abbreviated as “Spline-Trans” (Yuan et al., 2024), the penalized MLE method for the PH model with linear covariate effects abbreviated as “Penalized PH” (Zhao et al., 2020), and the nonparametric MLE method for the transformation model with linear covariate effects abbreviated as “NPMLE-Trans” (Zeng et al., 2016). For each $i = 1, \dots, n$, the partially linear additive transformation model in Yuan et al. (2024) specifies the cumulative hazard function of T_i given \mathbf{X}_i and \mathbf{W}_i as $\Lambda(t \mid \mathbf{X}_i, \mathbf{W}_i) = G\{\Lambda(t) \exp\{\boldsymbol{\beta}^\top \mathbf{X}_i + \sum_{k=1}^K \phi_k(W_{ik})\}\}$, where $\boldsymbol{\beta}$ is a vector of unknown regression coefficients, W_{ik} is the k th component of \mathbf{W}_i , and ϕ_k is an unknown function with $k = 1, \dots, K$. In Yuan et al. (2024)’s approach, B -splines were used to estimate each $\phi_k(W_{ik})$.

The results obtained from the above four methods on the regression parameter estimates are also summarized in Table 1. In the case of linear covariate effects (e.g., Case 1 and Case 4), “Penalized PH” and “NPMLE-Trans” perform satisfactorily and are comparable

Table 1: Simulation results for the regression parameter estimates under the PH model. Results include the estimation bias (Bias), the sample standard error (SSE) of the estimates, the average of the standard error estimates (SEE), and the 95% coverage probability (CP95).

Case	n	par.	Proposed method				Deep PH		Spline-Trans		Penalized PH		NPMLE-Trans	
			Bias	SSE	SEE	CP95	Bias	SSE	Bias	SSE	Bias	SSE	Bias	SSE
1	500	β_1	0.011	0.086	0.094	0.985	0.037	0.098	-0.002	0.145	-0.014	0.086	0.008	0.086
		β_2	-0.009	0.167	0.176	0.965	-0.020	0.186	-0.038	0.186	0.069	0.206	-0.008	0.168
	1000	β_1	0.018	0.059	0.063	0.965	0.017	0.060	0.030	0.061	0.008	0.059	0.023	0.060
		β_2	-0.015	0.125	0.121	0.965	-0.010	0.125	-0.028	0.134	0.011	0.129	-0.021	0.125
2	500	β_1	-0.015	0.087	0.097	0.985	-0.026	0.091	0.019	0.129	-0.087	0.087	-0.067	0.084
		β_2	<0.001	0.171	0.180	0.975	0.037	0.177	-0.053	0.188	0.145	0.221	0.055	0.168
	1000	β_1	-0.004	0.062	0.065	0.960	-0.024	0.065	0.032	0.065	-0.069	0.064	-0.055	0.064
		β_2	0.016	0.124	0.120	0.955	0.028	0.118	-0.021	0.127	0.102	0.137	0.064	0.121
3	500	β_1	0.011	0.085	0.095	0.980	0.020	0.096	-0.007	0.134	-0.043	0.081	-0.022	0.081
		β_2	-0.004	0.172	0.178	0.960	-0.021	0.195	-0.025	0.190	0.105	0.221	0.024	0.174
	1000	β_1	0.013	0.062	0.064	0.955	0.009	0.059	0.010	0.065	-0.026	0.061	-0.011	0.061
		β_2	-0.002	0.119	0.121	0.970	-0.009	0.123	-0.003	0.124	0.050	0.129	0.014	0.117
4	500	β_1	0.056	0.096	0.096	0.930	0.049	0.095	0.106	0.115	0.001	0.090	0.023	0.089
		β_2	-0.035	0.150	0.171	0.970	0.069	0.175	-0.079	0.191	0.056	0.161	-0.001	0.143
	1000	β_1	0.020	0.060	0.060	0.959	0.030	0.065	0.041	0.063	-0.005	0.054	0.004	0.054
		β_2	-0.013	0.108	0.108	0.964	0.048	0.122	-0.033	0.119	0.025	0.105	0.005	0.102
5	500	β_1	-0.005	0.093	0.105	0.965	0.057	0.169	0.122	0.129	-0.075	0.088	-0.058	0.087
		β_2	0.009	0.168	0.192	0.985	-0.104	0.292	-0.119	0.223	0.135	0.196	0.066	0.159
	1000	β_1	-0.020	0.069	0.067	0.943	0.018	0.090	0.045	0.070	-0.080	0.057	-0.076	0.056
		β_2	0.031	0.138	0.119	0.953	-0.027	0.158	-0.038	0.132	0.106	0.109	0.083	0.103
6	500	β_1	-0.003	0.093	0.103	0.944	0.052	0.161	0.019	0.116	-0.111	0.080	-0.092	0.080
		β_2	0.012	0.165	0.180	0.949	-0.100	0.277	-0.008	0.203	0.169	0.194	0.095	0.154
	1000	β_1	-0.035	0.060	0.064	0.927	0.012	0.099	-0.058	0.059	-0.123	0.049	-0.115	0.049
		β_2	0.037	0.107	0.111	0.938	-0.053	0.165	0.058	0.121	0.144	0.109	0.118	0.100

* Note: “Proposed method” denotes the proposed deep regression approach, “Deep PH ” refers to the deep learning approach for the partially linear PH model (Du et al., 2024), “Spline-Trans” refers to the sieve MLE approach for the partially linear additive transformation model (Yuan et al., 2024), “Penalized PH” refers to penalized MLE method for the PH model with linear covariate effects (Zhao et al., 2020), “NPMLE-Trans” refers to the nonparametric MLE method for the transformation model with linear covariate effects (Zeng et al., 2016).

Table 2: Simulation results for the relative error (RE) of $\hat{\phi}_{\alpha}$ over ϕ and the mean squared error (MSE) of the estimated survival function. Values of MSE in the table are multiplied by 100.

Case	n	Proposed method		Deep PH		Spline-Trans		Penalized PH		NPMLE-Trans	
		RE	MSE	RE	MSE	RE	MSE	RE	MSE	RE	MSE
1	500	0.314	0.267	0.405	0.511	1.739	0.984	0.294	0.254	0.236	0.510
	1000	0.230	0.131	0.309	0.349	1.824	0.323	0.196	0.112	0.170	0.229
2	500	0.515	0.739	0.640	1.226	1.037	0.790	0.855	1.679	0.854	1.879
	1000	0.423	0.477	0.518	0.873	0.740	0.309	0.837	1.558	0.841	1.686
3	500	0.728	0.545	0.769	0.725	1.812	2.013	0.985	0.881	1.012	1.160
	1000	0.571	0.314	0.599	0.481	1.516	1.383	0.975	0.797	0.985	0.927
4	500	0.477	0.625	0.516	1.163	2.044	1.389	0.365	0.412	0.320	0.718
	1000	0.313	0.285	0.421	1.039	1.947	0.545	0.263	0.206	0.216	0.337
5	500	0.358	1.606	0.545	3.212	1.574	0.900	0.430	1.803	0.426	2.489
	1000	0.292	0.984	0.421	2.515	1.407	0.369	0.415	1.573	0.415	1.889
6	500	0.556	1.883	0.749	3.365	1.126	3.903	0.767	2.767	0.767	3.168
	1000	0.488	1.262	0.630	2.603	1.078	3.199	0.761	2.545	0.763	2.740

* Note: “Proposed method” denotes the proposed deep regression approach, “Deep PH ” refers to the deep learning approach for the partially linear PH model (Du et al., 2024), “Spline-Trans” refers to the sieve MLE approach for the partially linear additive transformation model (Yuan et al., 2024), “Penalized PH” refers to penalized MLE method for the PH model with linear covariate effects (Zhao et al., 2020), “NPMLE-Trans” refers to the nonparametric MLE method for the transformation model with linear covariate effects (Zeng et al., 2016).

to the proposed method. This finding is anticipated since the model used in “Penalized PH” and “NPMLE-Trans” is correctly specified under the case of linear covariate effects. “Spline-Trans” yields significant estimation biases in Case 4 when the sample size is 500, partially because “Spline-Trans” suffers from the curse of dimensionality if the length of \mathbf{W} is considerable. Regarding the settings of nonlinear covariate effects, “Penalized PH” and “NPMLE-Trans” generally exhibit large estimation biases since the assumed models are misspecified. Although “Spline-Trans” is applicable to estimate a partially linear model, it can only accommodate a few nonlinear covariates in an additive form as suggested by Yuan et al. (2024). This fact and the curse of dimensionality restrict the empirical performance of “Spline-Trans” on estimating β sometimes (e.g., Cases 5 and 6). “Deep PH” exhibits considerable estimation biases in the settings of $n = 500$ and 10 nonlinear covariates (i.e., Cases 5 and 6). Such inferior performance arises partially because the estimate of cumulative hazard function cannot remain monotone with the optimization procedure of “Deep PH”.

To evaluate the prediction accuracy of the proposed deep regression method, we used the relative error (RE) of $\hat{\phi}$ over ϕ and the mean squared error (MSE) of the estimated survival function as in Zhong et al. (2022) and Sun and Ding (2023). In particular, RE is defined as

$$\text{RE}(\hat{\phi}) = \left[\frac{\frac{1}{n_1} \sum_{i=1}^{n_1} \left\{ \hat{\phi}(\mathbf{W}_i) - \phi(\mathbf{W}_i) \right\}^2}{\frac{1}{n_1} \sum_{i=1}^{n_1} \left\{ \phi(\mathbf{W}_i) \right\}^2} \right]^{1/2},$$

and MSE of the estimated survival function is defined as

$$\text{MSE}(\hat{S}) = \frac{1}{n_1} \sum_{i=1}^{n_1} \frac{1}{T_i} \int_0^{T_i} \left\{ S(t \mid \mathbf{X}_i, \mathbf{W}_i) - \hat{S}(t \mid \mathbf{X}_i, \mathbf{W}_i) \right\}^2 dt, \quad (6)$$

where $S(t \mid \mathbf{X}_i, \mathbf{W}_i) = \exp(-G[\Lambda(t) \exp\{\beta^\top \mathbf{X}_i + \phi(\mathbf{W}_i)\}])$, $\hat{S}(t \mid \mathbf{X}_i, \mathbf{W}_i) = \exp(-G[\hat{\Lambda}(t) \exp\{\hat{\beta}^\top \mathbf{X}_i + \hat{\phi}(\mathbf{W}_i)\}])$, and $\{T_i, \mathbf{X}_i, \mathbf{W}_i; i = 1, \dots, n_1\}$ is the test dataset with $n_1 = 0.2n$.

Smaller values of REs shown in Table 2 indicate a better prediction performance of the

proposed method over the “Deep PH” and “Spline-Trans”. “Deep PH” generally produces larger MSEs than the proposed method, especially under Cases 4–6. In addition, it can be observed that “Spline-Trans” can only yield comparable results to the proposed method under the additive models (e.g., Case 2 and Case 5) when the sample size is large. In more complex settings (e.g., Case 3 and Case 6), the proposed deep approach consistently outperforms the “Spline-Trans”. As for “Penalized PH” and “NPMLE-Trans”, they both yield conspicuously large REs and MSEs except for the cases of linear covariate effects (i.e., Case 1 and Case 4). The above comparison results all manifest the significant advantages of the proposed method in terms of prediction accuracy.

In Section S.3 of the supplementary materials, we conducted simulations under other regression models, such as the PO model. The results given in Tables S1 and S2 suggest similar conclusions as mentioned above regarding the comparisons of the proposed method, “Spline-Trans” and “NPMLE-Trans”. The performances of “deep PH” and “penalized PH” deteriorate remarkably due to using a misspecified PH model. This phenomenon further demonstrates the practical utility of developing a general deep regression model.

5 Application

We applied the proposed deep regression method to a set of interval-censored failure time data from the Alzheimer’s Disease Neuroimaging Initiative (ADNI) study initiated in 2004. This ADNI study recruited over 2,000 participants from North America, documenting their cognitive conditions categorized into three groups: cognitively normal, mild cognitive impairment (MCI), and Alzheimer’s disease (AD). In our analysis, we followed Li et al. (2017) and other researchers by concentrating on individuals who had experienced cognitive decline in the MCI group. Our primary objective is to investigate the crucial risk factors

for the progression of mild cognitive impairment to AD, thereby enhancing individuals' quality of life and extending their cognitive health span. The failure time of interest was defined as the duration from participant recruitment to the AD conversion. Since each participant was examined intermittently for the AD development, the AD occurrence time cannot be attained precisely and suffers from general interval censoring. In other words, the exact AD onset time of each participant is only known to fall into a time interval. The dataset consists of a total of 938 participants with 331 interval-censored observations and 579 right censored ones.

We focused on 14 potential risk factors for AD, consisting of a genetic covariate: **APOE ϵ 4** (coded as 0, 1, or 2 based on the number of APOE 4 alleles), four demographic covariates: **Age** (given in years), **Gender** (1 for male and 0 for female), **Education** (years of education), **Marry** (for married and 0 otherwise), and nine test scores, which are explained in Section S.4 of the supplementary materials due to the space restriction. We randomly divided the entire data into a training dataset consisting of 742 individuals and a test dataset of 196 observations, where the latter was used to evaluate the prediction performance and select the optimal hyperparameters as well as the optimal transformation function of the proposed method.

Note that **APOE ϵ 4**, **Age** and **Gender** were reported as crucial factors for developing AD in many studies, including Sun et al. (2021), Mielke et al. (2022) and Livingston et al. (2023). Our analysis attempted to investigate these three potential risk factors while controlling for other variables. Therefore, we included **APOE ϵ 4**, **Age** and **Gender** in the linear term of model (1), aiming to examine their effects quantitatively on the progression of AD in individuals with mild cognitive impairment. Other covariates were treated as control variables adjusted in the regression model. That is, we assumed that the failure time of interest followed the

partially linear transformation model with the conditional hazard function:

$$\Lambda(t \mid \mathbf{X}, \mathbf{W}) = G[\Lambda(t) \exp\{X_1\beta_1 + X_2\beta_2 + X_3\beta_3 + \phi(\mathbf{W})\}],$$

where $G(x) = \log(1 + rx)/r$ with $r \geq 0$, $X_1 = \text{Age}$, $X_2 = \text{Gender}$, $X_3 = \text{APOE}\epsilon 4$ and \mathbf{W} includes all the aforementioned covariates except X_1 , X_2 and X_3 . Note that the above transformation model with $r = 0$ (i.e., $G(x) = x$) corresponds to the partially linear PH model while setting $r = 1$ in the above model yields the partially linear PO model.

We used cubic splines to approximate $\Lambda(\cdot)$ and considered a sequence of integers ranging from 1 to 8 to determine the optimal number of interior knots. These interior knots were placed equally spaced quantiles between the minimum and maximum observation times. For the transformation function $G(\cdot)$, we let r vary from 0 to 5 with an increment of 0.1. In constructing the neural network, as in the simulation studies, we considered 2 or 3 hidden layers, 50 neurons in each hidden layer, and the SeLU activation function. We set the tuning parameter in the L_1 penalty to 0.1, 0.05 or 0.01 and the learning rate to 10^{-3} or 5×10^{-3} to train the constructed network. The mini-batch size in the SGD algorithm was set to 30. The neural network was trained for 20 epochs during each iteration of the proposed EM algorithm. Meanwhile, we used the dropout regularization with a rate of 0.1 to prevent overfitting. To measure the prediction performance of the proposed method, we utilized an integrated Brier score (IBS) calculated on the test data. The explicit definition of IBS can be found in Section S.4 of the supplementary materials. A smaller value of IBS corresponds to a better prediction performance. The analysis showed that the partially linear model with $r = 2.6$ was optimal.

Table 3 presents the analysis results for parametric covariate effects with the proposed deep and four comparative methods described in the simulations, including “Deep PH ” (Du et al., 2024), “Penalized PH” (Zhao et al., 2020), “Spline-Trans” (Yuan et al., 2024),

and “NPMLE-Trans” (Zeng et al., 2016). Results include the regression parameter estimates (EST), the estimated standard errors (SE), and p -values. Specifically, the SEs of the proposed deep method and “NPMLE-Trans” were obtained via the profile likelihood method, while the SEs of “Penalized PH” and “Spline-Trans” were calculated using nonparametric bootstrapping with a bootstrap size 100. The results obtained from the proposed deep learning method with $r = 2.6$, as presented in Table 3, reveal that males exhibit a significantly higher risk of developing AD compared to females. The presence of the **APOE ϵ 4** allele demonstrates a notably positive association with the risk of AD, suggesting that carrying the **APOE ϵ 4** allele increases the hazard of developing AD. In particular, individuals carrying two **APOE ϵ 4** alleles are at an even greater risk than those carrying only one allele. Furthermore, among individuals who had already experienced cognitive decline, **Age** is also a significant risk factor for AD by our method; being older represents a higher risk of developing AD. The proposed method with $r = 0$ (PH model) or 1 (PO model) leads to the same conclusions as the optimal model. Regarding the results of the four comparative methods, compared to the proposed method, the most notable difference is that the comparative methods all recognized **Age** as insignificant. This conclusion may be erroneous since age has been widely acknowledged as one of the most significant influential factors for AD (e.g., James et al., 2019; Livingston et al., 2023).

In Section S.4 of the supplementary materials, we conducted a 5-fold cross-validation to investigate the prediction performance of the proposed deep method. Figure S1 presents the obtained IBS values across all folds under the proposed deep regression method with the optimal model ($r = 2.6$) and the above comparative methods. It shows that the proposed method leads to the smallest IBS value except for the first fold, confirming our method’s powerful prediction ability.

Table 3: Analysis results of the ADNI data. “EST” and “SE” denote the regression parameter estimate and its standard error estimate, respectively.

Method	Age			Gender			APOE ϵ 4		
	EST	SE	p -value	EST	SE	p -value	EST	SE	p -value
Proposed method ($r=2.6$)	0.089	0.029	0.002	0.434	0.045	< 0.001	0.753	0.045	< 0.001
Proposed method ($r=0$)	0.092	0.029	0.002	0.378	0.048	< 0.001	0.374	0.045	< 0.001
Proposed method ($r=1$)	0.108	0.032	0.001	0.464	0.034	< 0.001	0.568	0.034	< 0.001
Deep PH	0.067	0.111	0.543	0.384	0.172	0.025	0.319	0.114	0.005
Penalized PH	0	0.079	1.000	0.320	0.199	0.108	0.317	0.124	0.011
Spline-Trans ($r=2.6$)	-0.089	0.169	0.600	0.761	0.350	0.030	0.742	0.264	0.005
Spline-Trans ($r=0$)	0.342	0.403	0.396	0.336	0.469	0.474	1.229	0.402	0.002
Spline-Trans ($r=1$)	0.040	0.141	0.777	0.596	0.286	0.037	0.290	0.187	0.121
NPMLE-Trans ($r=2.6$)	0.062	0.121	0.609	0.524	0.241	0.030	0.671	0.164	< 0.001
NPMLE-Trans ($r=0$)	0.123	0.073	0.092	0.422	0.145	0.004	0.388	0.093	< 0.001
NPMLE-Trans ($r=1$)	0.106	0.096	0.270	0.482	0.198	0.015	0.536	0.129	< 0.001

* Note: “Proposed method” denotes the proposed deep regression approach, “Deep PH ” refers to the deep learning approach for the partially linear PH model (Du et al., 2024), “Spline-Trans” refers to the sieve MLE approach for the partially linear additive transformation model (Yuan et al., 2024), “Penalized PH” refers to penalized MLE method for the PH model with linear covariate effects (Zhao et al., 2020), “NPMLE-Trans” refers to the nonparametric MLE method for the transformation model with linear covariate effects (Zeng et al., 2016). $r = 0$ and $r = 1$ correspond to the PH and PO models, respectively.

6 Discussion and Concluding Remarks

Inspired by DNN’s powerful approximation ability, this study proposed a novel deep regression approach for analyzing interval-censored data with a class of partially linear transformation models. Our proposed method leveraged the spirit of sieve estimation, in which the nonparametric component of the model was approximated by DNN. Since incorporating deep learning into time-to-event analysis is relatively new, it is easy to envision some potential future directions. For example, in practical applications, the failure times of interest are often accompanied by complex features (e.g., left truncation and competing risks (Shen et al., 2009; Mao and Lin , 2017) or garnered from intractable sampling strategies, such as group testing and case-cohort design (Zhou et al., 2017; Li et al., 2024). Thus, generalizations of the proposed deep regression approach to account for the settings above warrant future research. Furthermore, multivariate interval-censored data arise frequently in many real-life studies, where each individual may undergo multiple events of interest that suffer from interval censoring (Zeng et al., 2017; Sun et al., 2022). Naturally, the multiple event times of the same individual are correlated, which poses considerable challenges in parameter estimation and theoretical development. Therefore, meaningful future work is to explore some deep learning methods tailored to multivariate interval-censored data.

Acknowledgment

This research was partly supported by the National Natural Science Foundation of China (12471251), and the Research Grant Council of the Hong Kong Special Administrative Region (14301918, 14302519).

References

- Bauer, B., Kohler, M.(2019). On deep learning as a remedy for the curse of dimensionality in nonparametric regression. *The Annals of Statistics* **47**(4), 2261 – 2285.
- Chen, D., Li, J., Xu, K.(2020). Arelu: Attention-based rectified linear unit. *arXiv: 2006.13858*.
- Chen, K., Jin, Z.(2006). Partial Linear Regression Models for Clustered Data. *Journal of the American Statistical Association* **101**(473), 195–204.
- Cybenko, G.(1989). Approximation by superpositions of a sigmoidal function. *Mathematics of Control, Signals and Systems* **2**,303–314.
- Devlin, J., Chang, M.W., Lee, K., Toutanova, K.(2019). BERT: Pre-training of Deep Bidirectional Transformers for Language Understanding. *arXiv: 1810.04805*.
- Du, M., Wu, Q., Tong, X., Zhao, X.(2024). Deep learning for regression analysis of interval-censored data. *Electronic Journal of Statistics* **18**(2),4292–4321.
- Dubey, S.R., Singh, S.K., Chaudhuri, B.B.(2022). Activation functions in deep learning: A comprehensive survey and benchmark. *Neurocomputing* **503**,92–108.
- Fan, J., Gijbels, I., King, M. (1997). Local likelihood and local partial likelihood in hazard regression. *The Annals of Statistics* **25**(4), 1661–1690.
- Faraggi, D., Simon, R. (1995). A neural network model for survival data. *Statistics in Medicine* **14**(1), 73–82.
- Glorot, X., Bengio, Y. (2010). Understanding the difficulty of training deep feedforward

- neural networks. *Proceedings of the 13th International Conference on Artificial Intelligence and Statistics* **9**, 249–256.
- Goodfellow, I., Bengio, Y., Courville, A. (2016). *Deep learning*, MIT press.
- He, K., Zhang, X., Ren, S., Sun, J. (2015). Delving deep into rectifiers: Surpassing human-level performance on imagenet classification. *2015 IEEE International Conference on Computer Vision* **9**, 1026–1034.
- Hornik, K., Stinchcombe, M., White, H. (1989). Multilayer feedforward networks are universal approximators. *Neural Networks* **2**(5), 359–366.
- Huang, J. (1996). Efficient estimation for the proportional hazards model with interval censoring. *The Annals of Statistics* **24**(2), 540–568.
- Huang, J. (1999). Efficient Estimation of the Partly Linear Additive Cox Model. *The Annals of Statistics* **27**(5), 1536–1563.
- James, S.L., Theadom, A., Ellenbogen, R.G., et al. (2019). Global, regional, and national burden of traumatic brain injury and spinal cord injury, 1990-2016: a systematic analysis for the Global Burden of Disease Study 2016. *Lancet Neurology* **18**(1), 56–87.
- Katzman, J.L., Shaham, U., Cloninger, A., Bates, J., Jiang, T., Kluger, Y. (2018). DeepSurv: personalized treatment recommender system using a Cox proportional hazards deep neural network. *BMC Medical Research Methodology* **18**, 24.
- Klambauer, G., Unterthiner, T., Mayr, A., Hochreiter, S. (2017). Self-Normalizing Neural Networks. *arXiv: 1706.02515*.
- Kosorok, M.R., Lee, B.L., Fine, J.P. (2004). Robust inference for univariate proportional hazards frailty regression models. *The Annals of Statistics* **32**(10), 1448–1491.

- Kvamme, H., Borgan, O., Scheel, I. (2019). Time-to-event prediction with neural networks and Cox regression. *Journal of Machine Learning Research* **20**(129), 1–30.
- Lee, C.Y., Wong, K.Y., Lam, K.F., Xu, J. (2022). Analysis of clustered interval-censored data using a class of semiparametric partly linear frailty transformation models. *Biometrics* **78**(1), 165–178.
- Li, K., Chan, W., Doody, R.S., Quinn, J., Luo, S., Initiative, A.D.N., et al. (2017). Prediction of conversion to Alzheimer’s disease with longitudinal measures and time-to-event data. *Journal of Alzheimer’s Disease* **58**(2), 361–371.
- Li, S., Hu, T., Wang, L., McMahan, C.S., Tebbs, J.M. (2024). Regression analysis of group-tested current status data. *Biometrika* **111**(3), 1047–1061.
- Li, S., Peng, L. (2023). Instrumental variable estimation of complier causal treatment effect with interval-censored data. *Biometrics* **79**(1), 253–263.
- Livingston, G., Huntley, J., Sommerlad, A. (2023). Dementia prevention, intervention, and care: 2020 report of the Lancet Commission. *Lancet* **402**(10408), 1132–1132.
- Lu, M., McMahan, C.S. (2018). A partially linear proportional hazards model for current status data. *Biometrics* **74**(4), 1240–1249.
- Lu, M., Zhang, Y., Huang, J. (2007). Estimation of the Mean Function with Panel Count Data Using Monotone Polynomial Splines. *Biometrika* **94**(3), 705–718.
- Lu, W., Zhang, H.H. (2010). On estimation of partially linear transformation models. *Journal of the American Statistical Association* **105**(490), 683–691.
- Mao, L., Lin, D.Y. (2017). Efficient estimation of semiparametric transformation models

- for the cumulative incidence of competing risks. *Journal of the Royal Statistical Society: Series B* **79**(2), 573–587.
- Mielke, M.M., Aggarwal, N.T., Vila-Castelar, C., et al.(2022). Consideration of sex and gender in Alzheimer’s disease and related disorders from a global perspective. *Alzheimer’s & Dementia* **18**(2), 1–18.
- Ramsay, J.O. (1988). Monotone regression splines in action. *Statistical Science* **32**, 425–441.
- Ren, K., Qin, J., Zheng, L., Yang, Z., Zhang, W., Qiu, L., Yu, Y. (2019). Deep recurrent survival analysis. *AAAI Conference on Artificial Intelligence* **33**(01), 4798–4805.
- Ren, S., He, K., Girshick, R., Sun, J. (2017). Faster R-CNN: Towards real-time object detection with region proposal networks. *IEEE Transactions on Pattern Analysis and Machine Intelligence* **39**(6), 1137–1149.
- Schmidt-Hieber, J. (2020). Nonparametric regression using deep neural networks with ReLU activation function. *The Annals of Statistics* **48**(4), 1875 – 1897.
- Shen, Y., Ning, J., Qin, J. (2009). Analyzing length-biased data with semiparametric transformation and accelerated failure time models. *Journal of the American Statistical Association* **104**(487), 1192–1202.
- Silver, D., Schrittwieser, J., Simonyan, K., Antonoglou, I., Huang, A., Guez, A., Hubert, T., Baker, L., Lai, M., Bolton, A., et al. (2017). Mastering the game of go without human knowledge. *Nature* **550**(7676), 354–359.
- Srivastava, N., Hinton, G., Krizhevsky, A., Sutskever, I., Salakhutdinov, R. (2014). Dropout: a simple way to prevent neural networks from overfitting. *Journal of Machine Learning Research* **15**(1), 1929–1958.

- Sun, J. (2006). *The Statistical Analysis of Interval-Censored Failure Time Data*, Springer, New York.
- Sun, L., Li, S., Wang, L., Song, X., Sui, X. (2022). Simultaneous variable selection in regression analysis of multivariate interval-censored data. *Biometrics* **78**(4), 1402–1413.
- Sun, R., Zhou, X., Song, X. (2021). Bayesian Causal Mediation Analysis with Latent Mediators and Survival Outcome. *Structural Equation Modeling: A Multidisciplinary Journal* **28**(5), 778–790.
- Sun, T., Ding, Y. (2023). Neural network on interval-censored data with application to the prediction of Alzheimer’s disease. *Biometrics* **79**(3), 2677–2690.
- Sun, Y., Kang, J., Haridas, C., Mayne, N., Potter, A., Yang, C.F., Christiani, D.C., Li, Y. (2024). Penalized deep partially linear cox models with application to CT scans of lung cancer patients. *Biometrics* **80**(1), ujad024.
- Telgarsky, M. (2015). Representation benefits of deep feedforward networks. *arXiv: 1509.08101*.
- Tong, J., Zhao, X. (2022). Deep survival algorithm based on nuclear norm. *Journal of Statistical Computation and Simulation* **92**(9), 1964–1976.
- Wang, L., McMahan, C.S., Hudgens, M.G., Qureshi, Z.P. (2016). A flexible, computationally efficient method for fitting the proportional hazards model to interval-censored data. *Biometrics* **72**(1), 222–231.
- Wu, Q., Tong, X., Zhao, X. (2024). Deep partially linear cox model for current status data. *Biometrics* **80**(2), ujae024.

- Xie, Y., Yu, Z. (2021). Promotion time cure rate model with a neural network estimated nonparametric component. *Statistics in Medicine* **40**(15),3516–3532.
- Yuan, C., Zhao, S., Li, S., Song, X. (2024). Sieve Maximum Likelihood Estimation of Partially Linear Transformation Models With Interval-Censored Data. *Statistics in Medicine* **43**(30), 5765 – 5776.
- Zeng, D., Gao, F., Lin, D.Y. (2017). Maximum likelihood estimation for semiparametric regression models with multivariate interval-censored data. *Biometrika* **104**(3), 505–525.
- Zeng, D., Lin, D.Y. (2006). Efficient estimation of semiparametric transformation models for counting processes. *Biometrika* **93**(3), 627–640.
- Zeng, D., Mao, L., Lin, D. (2016). Maximum likelihood estimation for semiparametric transformation models with interval-censored data. *Biometrika* **103**(2), 253–271.
- Zhang, Y., Hua, L., Huang, J. (2010). A spline-based semiparametric maximum likelihood estimation method for the Cox model with interval-censored data. *Scandinavian Journal of Statistics* **37**(2), 338–354.
- Zhao, H., Wu, Q., Li, G., Sun, J. (2020). Simultaneous estimation and variable selection for interval-censored data with broken adaptive ridge regression. *Journal of the American Statistical Association* **115**(529), 204-216.
- Zhong, Q., Mueller, J., Wang, J.L. (2022). Deep learning for the partially linear Cox model. *The Annals of Statistics* **50**(3), 1348–1375.
- Zhou, Q., Zhou, H., Cai, J. (2017). Case-cohort studies with interval-censored failure time data. *Biometrika* **104**(1), 17–29.

Supplementary Materials for “Interpretable Deep Regression Models with Interval-Censored Failure Time Data”

Changhui Yuan

School of Mathematics, Jilin University

and

Shishun Zhao

School of Mathematics, Jilin University

and

Shuwei Li

School of Economics and Statistics, Guangzhou University

and

Xinyuan Song

Department of Statistics, Chinese University of Hong Kong

and

Zhao Chen

School of Data Science, Fudan University

Section S.1: Estimation Procedure

We propose an EM algorithm to conduct the sieve maximum likelihood estimation based on likelihood (4) of the main manuscript. We first introduce a three-stage data augmentation procedure to construct the complete data likelihood with a tractable form. By considering the class of frailty-induced logarithmic transformations introduced in Section 2.1 of the main manuscript, the observed data likelihood (4) of the main manuscript can

be equivalently formulated as

$$\begin{aligned}
& \mathcal{L}_1(\boldsymbol{\beta}, \boldsymbol{\gamma}, \boldsymbol{\alpha}) \\
&= \prod_{i=1}^n \int_0^\infty \{1 - \exp\{-\Lambda_\gamma(R_i) \exp\{\boldsymbol{\beta}^\top \mathbf{X}_i + \phi_\alpha(\mathbf{W}_i)\}\eta_i\}\}^{\delta_{L,i}} \\
&\quad \times \left(\exp\{-\Lambda_\gamma(L_i) \exp\{\boldsymbol{\beta}^\top \mathbf{X}_i + \phi_\alpha(\mathbf{W}_i)\}\eta_i\} - \exp\{-\Lambda_\gamma(R_i) \exp\{\boldsymbol{\beta}^\top \mathbf{X}_i + \phi_\alpha(\mathbf{W}_i)\}\eta_i\} \right)^{\delta_{L,i}} \\
&\quad \times \exp\{-\Lambda_\gamma(L_i) \exp\{\boldsymbol{\beta}^\top \mathbf{X}_i + \phi_\alpha(\mathbf{W}_i)\}\eta_i\}^{\delta_{R,i}} f(\eta_i | r) d\eta_i.
\end{aligned} \tag{S1}$$

For subject i , define $t_{i2} = R_i(\delta_{L,i} = 1) + L_i(\delta_{R,i} = 1)$ if $\delta_{L,i} = 0$, and $t_{i1} = R_i(\delta_{L,i} = 1) + L_i(\delta_{L,i} = 0)$. We introduce two independent Poisson random variables: $Z_i \sim Pois(\Lambda_\gamma(t_{i1}) \exp\{\boldsymbol{\beta}^\top \mathbf{X}_i + \phi_\alpha(\mathbf{W}_i)\}\eta_i)$ and $Y_i \sim Pois(\{\Lambda_\gamma(t_{i2}) - \Lambda_\gamma(t_{i1})\} \exp\{\boldsymbol{\beta}^\top \mathbf{X}_i + \phi_\alpha(\mathbf{W}_i)\}\eta_i)$, where $Pois(\nu)$ indicates the Poisson distribution with mean ν . Moreover, by the spline representation of $\Lambda_\gamma(t)$, we decompose Z_i and Y_i as $Z_i = \sum_{l=1}^{L_n} Z_{il}$ and $Y_i = \sum_{l=1}^{L_n} Y_{il}$, where $Z_{i1}, \dots, Z_{iL_n}, Y_{i1}, \dots, Y_{iL_n}$ are independent Poisson random variables, the mean of Z_{il} is $\gamma_l M_l(t_{i1}) \exp\{\boldsymbol{\beta}^\top \mathbf{X}_i + \phi_\alpha(\mathbf{W}_i)\}\eta_i$, and the mean of Y_{il} is $\gamma_l \{M_l(t_{i2}) - M_l(t_{i1})\} \exp\{\boldsymbol{\beta}^\top \mathbf{X}_i + \phi_\alpha(\mathbf{W}_i)\}\eta_i$ for $l = 1, \dots, L_n$. Then, the likelihood (S1) can be equivalently expressed as

$$\begin{aligned}
\mathcal{L}_2(\boldsymbol{\beta}, \boldsymbol{\gamma}, \boldsymbol{\alpha}) &= \prod_{i=1}^n \int_0^\infty P\left(\sum_{l=1}^{L_n} Z_{il} > 0\right)^{\delta_{L,i}} P\left(\sum_{l=1}^{L_n} Z_{il} = 0, \sum_{l=1}^{L_n} Y_{il} > 0\right)^{\delta_{L,i}} \\
&\quad \times P\left(\sum_{l=1}^{L_n} Z_{il} = 0, \sum_{l=1}^{L_n} Y_{il} = 0\right)^{\delta_{R,i}} f(\eta_i | r) d\eta_i.
\end{aligned}$$

Let $p(A | \tau)$ represent the probability mass function of a Poisson random variable A with mean τ . Treating all latent variables as observable, the complete-data likelihood is

$$\begin{aligned}
\mathcal{L}_c(\boldsymbol{\beta}, \boldsymbol{\gamma}, \boldsymbol{\alpha}) &= \prod_{i=1}^n \prod_{l=1}^{L_n} p(Z_{il} | \gamma_l M_l(t_{i1}) \exp\{\boldsymbol{\beta}^\top \mathbf{X}_i + \phi_\alpha(\mathbf{W}_i)\}\eta_i) \\
&\quad \times p(Y_{il} | \gamma_l \{M_l(t_{i2}) - M_l(t_{i1})\} \exp\{\boldsymbol{\beta}^\top \mathbf{X}_i + \phi_\alpha(\mathbf{W}_i)\}\eta_i)^{\delta_{L,i} + \delta_{R,i}} f(\eta_i | r),
\end{aligned} \tag{S2}$$

with constraints $\sum_{l=1}^{L_n} Z_{il} > 0$ if $\delta_{L,i} = 1$, $\sum_{l=1}^{L_n} Z_{il} = 0$ and $\sum_{l=1}^{L_n} Y_{il} > 0$ if $\delta_{L,i} = 1$, and $\sum_{l=1}^{L_n} Z_{il} = 0$ and $\sum_{l=1}^{L_n} Y_{il} = 0$ if $\delta_{R,i} = 1$.

In the E-step of the algorithm, we calculate the conditional expectation of $\log\{\mathcal{L}_c(\boldsymbol{\beta}, \boldsymbol{\gamma}, \boldsymbol{\alpha})\}$ with respect to all latent variables, given the observed data and the m th parameter updates denoted by $(\boldsymbol{\beta}^{(m)}, \boldsymbol{\gamma}^{(m)}, \boldsymbol{\alpha}^{(m)})$. In particular, $(\boldsymbol{\beta}^{(0)}, \boldsymbol{\gamma}^{(0)}, \boldsymbol{\alpha}^{(0)})$ denotes the initial value of $(\boldsymbol{\beta}, \boldsymbol{\gamma}, \boldsymbol{\alpha})$. After excluding some terms that are free of unknown parameters, this step leads to the following objective function:

$$\begin{aligned} Q(\boldsymbol{\beta}, \boldsymbol{\gamma}, \boldsymbol{\alpha}; \boldsymbol{\beta}^{(m)}, \boldsymbol{\gamma}^{(m)}, \boldsymbol{\alpha}^{(m)}) &= \sum_{i=1}^n \sum_{l=1}^{L_n} \left(\{\log \gamma_l + \boldsymbol{\beta}^\top \mathbf{X}_i + \phi_{\boldsymbol{\alpha}}(\mathbf{W}_i)\} \{E(Z_{il}) + (\delta_{L,i} + \delta_{R,i})E(Y_{il})\} \right. \\ &\quad \left. - \gamma_l \exp\{\boldsymbol{\beta}^\top \mathbf{X}_i + \phi_{\boldsymbol{\alpha}}(\mathbf{W}_i)\} E(\eta_i) \{(\delta_{L,i} + \delta_{R,i})M_l(R_i) + \delta_{R,i}M_l(L_i)\} \right). \end{aligned}$$

For notational simplicity, we will ignore some arguments, including the current parameter update and observed data, in the below conditional expectations. Let $\Lambda_{\boldsymbol{\gamma}}^{(m)}(t) = \sum_{l=1}^{L_n} \gamma_l^{(m)} M_l(t)$ and $\mathcal{U}_i^{(m)}(t) = \Lambda_{\boldsymbol{\gamma}}^{(m)}(t) \exp\{\mathbf{X}_i^\top \boldsymbol{\beta}^{(m)} + \phi_{\boldsymbol{\alpha}}^{(m)}(\mathbf{W}_i)\}$, where m is a non-negative integer. At the m th iteration of the proposed algorithm, by utilizing the law of iterated expectations and the facts that $Z_i = \sum_{l=1}^{L_n} Z_{il}$ and $Y_i = \sum_{l=1}^{L_n} Y_{il}$, we have

$$E(Z_{il}) = \frac{\gamma_l^{(m)} M_l(R_i)}{\Lambda_{\boldsymbol{\gamma}}^{(m)}(R_i)} E(Z_i),$$

and

$$E(Y_{il}) = \frac{\gamma_l^{(m)} M_l(R_i) - \gamma_l^{(m)} M_l(L_i)}{\Lambda_{\boldsymbol{\gamma}}^{(m)}(R_i) - \Lambda_{\boldsymbol{\gamma}}^{(m)}(L_i)} E(Y_i).$$

In addition, given η_i , the conditional expectations of Z_i and Y_i are

$$E(Z_i | \eta_i) = \frac{\mathcal{U}_i^{(m)}(R_i) \eta_i \delta_{L,i}}{1 - \exp\{-\mathcal{U}_i^{(m)}(R_i) \eta_i\}},$$

and

$$E(Y_i | \eta_i) = \frac{\{\mathcal{U}_i^{(m)}(R_i) \eta_i - \mathcal{U}_i^{(m)}(L_i) \eta_i\} \delta_{L,i}}{1 - \exp\{\mathcal{U}_i^{(m)}(L_i) \eta_i - \mathcal{U}_i^{(m)}(R_i) \eta_i\}},$$

respectively. Again, with the law of iterated expectations, the conditional expectations of Z_i and Y_i are given by

$$E(Z_i) = E_{\eta_i} \{E(Z_i | \eta_i)\} = \frac{\mathcal{U}_i^{(m)}(R_i) \delta_{L,i}}{1 - \exp\{-G[\mathcal{U}_i^{(m)}(R_i)]\}},$$

and

$$\begin{aligned}
E(Y_i) &= E_{\eta_i} \{E(Y_i | \eta_i)\} \\
&= \int_0^\infty \frac{\{\mathcal{U}_i^{(m)}(R_i)\eta_i - \mathcal{U}_i^{(m)}(L_i)\eta_i\} \delta_{I,i}}{1 - \exp\{\mathcal{U}_i^{(m)}(L_i)\eta_i - \mathcal{U}_i^{(m)}(R_i)\eta_i\}} \\
&\quad \times \frac{\exp\{-\mathcal{U}_i^{(m)}(L_i)\eta_i\} - \exp\{-\mathcal{U}_i^{(m)}(R_i)\eta_i\}}{\exp\{-G[\mathcal{U}_i^{(m)}(L_i)]\} - \exp\{-G[\mathcal{U}_i^{(m)}(R_i)]\}} f(\eta_i | r) d\eta_i,
\end{aligned}$$

respectively. Specifically, the numerical Gauss-Laguerre method can be used to compute the aforementioned integral that lacks a closed form. By using the Bayesian theorem, the conditional expectation of η_i takes the form

$$\begin{aligned}
E(\eta_i) &= \frac{\delta_{L,i} \{1 - (1 + r\mathcal{U}_i^{(m)}(R_i))^{-\frac{1+r}{r}}\}}{1 - \exp\{-G[\mathcal{U}_i^{(m)}(R_i)]\}} + \frac{\delta_{I,i} \{(1 + r\mathcal{U}_i^{(m)}(L_i))^{-\frac{1+r}{r}} - (1 + r\mathcal{U}_i^{(m)}(R_i))^{-\frac{1+r}{r}}\}}{\exp\{-G[\mathcal{U}_i^{(m)}(L_i)]\} - \exp\{-G[\mathcal{U}_i^{(m)}(R_i)]\}} \\
&\quad + \frac{\delta_{R,i} (1 + r\mathcal{U}_i^{(m)}(L_i))^{-\frac{1+r}{r}}}{\exp\{-G[\mathcal{U}_i^{(m)}(L_i)]\}}.
\end{aligned}$$

In the M-step of the algorithm, we proceed with updating the unknown parameter vector $\boldsymbol{\alpha}$ in the DNN. Specifically, we employ the popular mini-batch SGD algorithm to minimize the loss function $-Q(\boldsymbol{\beta}^{(m)}, \boldsymbol{\gamma}^{(m)}, \boldsymbol{\alpha}; \boldsymbol{\beta}^{(m)}, \boldsymbol{\gamma}^{(m)}, \boldsymbol{\alpha}^{(m)})$. In the $(m+1)$ th iteration, define $\phi_{\boldsymbol{\alpha}}^{(m+1)}(\mathbf{W}_i)$ as the $(m+1)$ th update of $\phi_{\boldsymbol{\alpha}}(\mathbf{W}_i)$ after obtaining $\boldsymbol{\alpha}^{(m+1)}$ for $i = 1, \dots, n$. Since we impose the constraint $E\{\phi(\mathbf{W})\} = 0$ to get an identifiable model, we redefine $\phi_{\boldsymbol{\alpha}}^{(m+1)}(\mathbf{W}_i)$ as $\phi_{\boldsymbol{\alpha}}^{(m+1)}(\mathbf{W}_i) - \frac{1}{n} \sum_{i=1}^n \phi_{\boldsymbol{\alpha}}^{(m+1)}(\mathbf{W}_i)$. Next, for each $l = 1, \dots, L_n$, by setting $\partial Q(\boldsymbol{\beta}, \boldsymbol{\gamma}, \boldsymbol{\alpha}^{(m+1)}; \boldsymbol{\beta}^{(m)}, \boldsymbol{\gamma}^{(m)}, \boldsymbol{\alpha}^{(m)}) / \partial \gamma_l = 0$, we can derive a closed-form update for γ_l that depends on the unknown $\boldsymbol{\beta}$:

$$\gamma_l^{(m+1)}(\boldsymbol{\beta}; \boldsymbol{\alpha}^{(m+1)}) = \frac{\sum_{i=1}^n E(Z_{il}) + (\delta_{I,i} + \delta_{R,i}) E(Y_{il})}{\sum_{i=1}^n \exp\{\boldsymbol{\beta}^\top \mathbf{X}_i + \phi_{\boldsymbol{\alpha}}^{(m+1)}(\mathbf{W}_i)\} E(\eta_i) \{(\delta_{L,i} + \delta_{I,i}) M_l(R_i) + \delta_{R,i} M_l(L_i)\}}.$$

Notably, given a nonnegative initial value for $\boldsymbol{\gamma}$, the proposed EM algorithm can automatically produce a nonnegative update of $\boldsymbol{\gamma}$ at each iteration, ensuring a monotone update of cumulative baseline hazard. This is a desirable feature of the proposed EM algorithm since it essentially avoids using the constrained optimization. By replacing each γ_l with $\gamma_l^{(m+1)}(\boldsymbol{\beta}; \boldsymbol{\alpha}^{(m+1)})$ in $Q(\boldsymbol{\beta}, \boldsymbol{\gamma}, \boldsymbol{\alpha}^{(m+1)}; \boldsymbol{\beta}^{(m)}, \boldsymbol{\gamma}^{(m)}, \boldsymbol{\alpha}^{(m)})$, we obtain the objective function for

β as follows:

$$Q_{\text{new}}(\beta) = \sum_{i=1}^n \sum_{l=1}^{L_n} \left(\{\beta^\top \mathbf{X}_i + \phi_{\alpha}^{(m+1)}(\mathbf{W}_i)\} \times \{E(Z_{il}) + (\delta_{I,i} + \delta_{R,i})E(Y_{il})\} \right. \\ \left. - \log \left[\sum_{j=1}^n \exp\{\beta^\top \mathbf{X}_j + \phi_{\alpha}^{(m+1)}(\mathbf{W}_j)\} E(\eta_j) \{(\delta_{L,j} + \delta_{I,j})M_l(R_j) + \delta_{R,j}M_l(L_j)\} \right] \right) \\ \times \{E(Z_{il}) + (\delta_{I,i} + \delta_{R,i})E(Y_{il})\}.$$

Then, the update of β can be readily obtained by applying the existing R optimization function, such as `nlm()`, with one step optimization to $Q_{\text{new}}(\beta)$.

In summary, the proposed algorithm proceeds with the following steps:

Step 1: Initialize $\beta^{(0)}$, $\gamma^{(0)}$, and $\alpha^{(0)}$. Set $m = 0$.

Step 2: In the $(m+1)$ th iteration, compute all the conditional expectations, $\{E(\eta_i), E(Z_{il}), E(Y_{il}); i = 1, \dots, n, l = 1, \dots, L_n\}$, based on $\beta^{(m)}$, $\gamma^{(m)}$, $\alpha^{(m)}$, and the observed data.

Step 3: Apply SGD to the loss function $-Q(\beta^{(m)}, \gamma^{(m)}, \alpha; \beta^{(m)}, \gamma^{(m)}, \alpha^{(m)})$, and obtain $\alpha^{(m+1)}$ and $\phi_{\alpha}^{(m+1)}(\mathbf{W}_i)$ subsequently for $i = 1, \dots, n$.

Step 4: Obtain $\beta^{(m+1)}$ by applying the one step optimization to $Q_{\text{new}}(\beta)$.

Step 5: Calculate $\gamma_l^{(m+1)} = \gamma_l(\beta^{(m+1)}; \alpha^{(m+1)})$ for $l = 1, \dots, L_n$. Increase m by 1.

Step 6: Repeat Step 2 to Step 5 until convergence is achieved.

In training the neural network, one often needs to tune several hyperparameters, including the number of hidden layers q , the number of neurons in each hidden layer, the tuning parameter in the penalty function, batch size, epoch size, dropout rate, and learning rate (Goodfellow et al., 2016). These hyperparameters can be tuned via a grid search, evaluating the log-likelihood value on a hold-out validation set during each training trial. Our experiences suggest that only the number of hidden layers, the tuning parameter in the penalty function and learning rate significantly impact the proposed method's performance. Thus, to save the computational burden, other insensitive hyperparameters are kept as fixed values in our numerical studies.

Section S.2: Proofs of Theorems 1–3

For notational simplicity, we define $\psi(\mathbf{U}) = \log \Lambda(R) + \phi(\mathbf{W})$, $\psi(\mathbf{V}) = \log \Lambda(L) + \phi(\mathbf{W})$, $\psi_0(\mathbf{U}) = \log \Lambda_0(R) + \phi_0(\mathbf{W})$ and $\psi_0(\mathbf{V}) = \log \Lambda_0(L) + \phi_0(\mathbf{W})$, where $\mathbf{U} = (R, \mathbf{W}^\top)^\top$ and $\mathbf{V} = (L, \mathbf{W}^\top)^\top$. Define $\Upsilon(\mathbf{x}, \mathbf{y}; \boldsymbol{\theta}) = G(\exp\{\boldsymbol{\beta}^\top \mathbf{x} + \psi(\mathbf{y})\})$ and $\Upsilon_0(\mathbf{x}, \mathbf{y}) = G(\exp\{\boldsymbol{\beta}_0^\top \mathbf{x} + \psi_0(\mathbf{y})\})$. The log-likelihood for a single subject is given by

$$\begin{aligned} \ell(\boldsymbol{\theta}) = & \delta_L \log[1 - \exp(-\Upsilon(\mathbf{X}, \mathbf{U}; \boldsymbol{\theta}))] + \delta_I \log[\exp(-\Upsilon(\mathbf{X}, \mathbf{V}; \boldsymbol{\theta})) - \exp(-\Upsilon(\mathbf{X}, \mathbf{U}; \boldsymbol{\theta}))] \\ & - \delta_R \Upsilon(\mathbf{X}, \mathbf{V}; \boldsymbol{\theta}). \end{aligned}$$

Let \mathbb{P}_n denote the empirical measure from n independent observations and \mathbb{P} denote the true probability measure. Specifically, for a measurable function f and a random variable X with the distribution F , $\mathbb{P}f$ is defined as $\int f(x)dF(x)$, and $\mathbb{P}_n f = \frac{1}{n} \sum_{i=1}^n f(X_i)$, where X_1, \dots, X_n are n independent realizations of X . Thus, $\mathbb{G}_n = \sqrt{n}(\mathbb{P}_n - \mathbb{P})$ is the corresponding empirical process. Let $\mathbb{M}(\boldsymbol{\theta}) = \mathbb{P}\{\ell(\boldsymbol{\theta})\}$ and $\mathbb{M}_n(\boldsymbol{\theta}) = \mathbb{P}_n\{\ell(\boldsymbol{\theta})\}$. Define $\boldsymbol{\theta}_n = (\boldsymbol{\beta}, \Lambda_\gamma, \phi_\alpha)$, $\mathcal{M}_B = \mathcal{M}(\mathcal{T}_n, d_M, B)$ and $\mathcal{F}_B = \mathcal{F}(s, q, \mathbf{h}, B)$ for some $B > 0$. In what follows, M denotes a general positive constant whose value may vary from place to place. Before proving Theorem 1, we need the following lemma.

Lemma 1. *Under conditions (C2)–(C4), the class $\{\ell(\boldsymbol{\theta}_n) : \boldsymbol{\theta}_n \in \mathcal{D} \times \mathcal{M}_B \times \mathcal{F}_B\}$ is Glivenko-Cantelli.*

Proof. For any $\varepsilon > 0$, we first know that there are $O(\varepsilon^{-p})$ number of brackets covering the compact set \mathcal{D} , such that the difference of any two $\boldsymbol{\beta}$ within the same bracket under Euclidean norm is at most ε . Consequently, the ε -bracketing number for the class $\{\boldsymbol{\beta}^\top \mathbf{X} : \boldsymbol{\beta} \in \mathcal{D}\}$ equipped by Euclidean norm is $O(\varepsilon^{-p})$ by Condition (C2). Similarly, there exist $O((B/\varepsilon)^{L_n})$ ε -brackets to cover $\{\boldsymbol{\gamma} \in \mathbb{R}^{L_n} : 0 \leq \gamma_l \leq B, l = 1, \dots, L_n\}$. Then, by Lemma 2.5 in (Van de Geer, 2000), the ε -bracketing number of \mathcal{M}_B equipped by Euclidean norm

is bounded by $O((B/\varepsilon)^{L_n})$ under Conditions (C3) and (C4).

To calculate the entropy of \mathcal{F}_B , we apply similar arguments as demonstrated in the proof of Lemma 6 of Zhong et al. (2022). Consider two neural networks ϕ_1 and $\phi_2 \in \mathcal{F}_B$, and let $\boldsymbol{\alpha}_{\phi_1} = (\boldsymbol{\omega}_{1,q}, \mathbf{v}_{1,q}, \dots, \boldsymbol{\omega}_{1,0}, \mathbf{v}_{1,0})$ and $\boldsymbol{\alpha}_{\phi_2} = (\boldsymbol{\omega}_{2,q}, \mathbf{v}_{2,q}, \dots, \boldsymbol{\omega}_{2,0}, \mathbf{v}_{2,0})$ be two sets of parameters related to ϕ_1 and ϕ_2 , respectively. We define the supremum norm of $(\boldsymbol{\alpha}_{\phi_1} - \boldsymbol{\alpha}_{\phi_2})$ as follows

$$\|\boldsymbol{\alpha}_{\phi_1} - \boldsymbol{\alpha}_{\phi_2}\|_\infty = \max_{j=0, \dots, q} (\|\boldsymbol{\omega}_{1,j} - \boldsymbol{\omega}_{2,j}\|_\infty \vee \|\mathbf{v}_{1,j} - \mathbf{v}_{2,j}\|_\infty).$$

Next, define the neural networks $\phi_{1,2}^j$ with parameters given by

$$\boldsymbol{\alpha}_{\phi_{1,2}^j} = (\boldsymbol{\omega}_{1,q}, \mathbf{v}_{1,q}, \dots, \boldsymbol{\omega}_{1,j+1}, \mathbf{v}_{1,j+1}, \boldsymbol{\omega}_{2,j}, \mathbf{v}_{2,j}, \dots, \boldsymbol{\omega}_{2,0}, \mathbf{v}_{2,0}), \text{ for } j = 0, \dots, q-1.$$

According to the neural network's definition, we have

$$\|\phi_{1,2}^j - \phi_{1,2}^{j-1}\|_\infty \leq \left(\prod_{k=j+1}^q h_k \right) \left\{ \|(\boldsymbol{\omega}_{2,j} - \boldsymbol{\omega}_{1,j}) \phi_j^*\|_\infty + \|\mathbf{v}_{1,j} - \mathbf{v}_{2,j}\|_\infty \right\},$$

where ϕ_j^* is a neural network with parameters $\boldsymbol{\alpha}_{\phi_j^*} = (\mathbf{I}_j, \mathbf{v}_{2,j}, \boldsymbol{\omega}_{2,j-1}, \mathbf{v}_{2,j-1}, \dots, \boldsymbol{\omega}_{2,0}, \mathbf{v}_{2,0})$ and \mathbf{I}_j represents an identity matrix. Since $\|\phi_j^*\|_\infty$ is bounded by $\prod_{k=0}^{j-1} (h_k + 1)$, we can conclude that

$$\|\phi_{1,2}^j - \phi_{1,2}^{j-1}\|_\infty \leq \left\{ \prod_{k=0}^q (h_k + 1) \right\} \|\boldsymbol{\alpha}_{\phi_1} - \boldsymbol{\alpha}_{\phi_2}\|_\infty.$$

Furthermore, we have

$$\|\phi_1 - \phi_2\|_\infty \leq \sum_{j=1}^q \|\phi_{1,2}^j - \phi_{1,2}^{j-1}\|_\infty \leq q \left\{ \prod_{k=0}^q (h_k + 1) \right\} \|\boldsymbol{\alpha}_{\phi_1} - \boldsymbol{\alpha}_{\phi_2}\|_\infty.$$

Given the fact that a neural network has at most $K_h = \sum_{j=0}^q (h_j + 1) h_{j+1}$ parameters, there are $\binom{K_h}{\tilde{s}}$ possible ways to select $\tilde{s} (\leq s)$ non-zero parameters. Define $K = q \prod_{k=0}^q (h_k + 1) \sum_{k=0}^q h_k h_{k+1}$. Therefore, for any $\varepsilon > 0$, the covering number $N(\varepsilon, \mathcal{F}_B, L_1(\mathbb{P}))$ satisfies

$$N(\varepsilon, \mathcal{F}_B, L_1(\mathbb{P})) \lesssim \sum_{\tilde{s}=1}^s \binom{K_h}{\tilde{s}} \left\{ \frac{q \prod_{k=0}^q (h_k + 1)}{\varepsilon} \right\}^{\tilde{s}} \lesssim \left(\frac{K}{\varepsilon} \right)^{s+1}.$$

By Theorem 2.7.11 in van der Vaart and Wellner (1996), we can obtain that the ε -bracketing number of \mathcal{F}_B equipped by L_2 -norm is bounded by $O((K/\varepsilon)^s)$.

For any $\boldsymbol{\theta}_1$ and $\boldsymbol{\theta}_2 \in \mathcal{D} \times \mathcal{M}_B \times \mathcal{F}_B$, by using Taylor series expansion, we get

$$\|\ell(\boldsymbol{\theta}_1) - \ell(\boldsymbol{\theta}_2)\|_{L_2}^2 \lesssim \|\boldsymbol{\beta}_1 - \boldsymbol{\beta}_2\|^2 + \|\Lambda_1 - \Lambda_2\|_{L_2}^2 + \|\phi_1 - \phi_2\|_{L_2}^2.$$

Then the ε -bracketing number of the class $\{\ell(\boldsymbol{\theta}_n) : \boldsymbol{\theta}_n \in \mathcal{D} \times \mathcal{M}_B \times \mathcal{F}_B\}$, equipped by $d(\boldsymbol{\theta}_1, \boldsymbol{\theta}_2)$ defined in Section 3 of the main paper, is bounded by $M(1/\varepsilon)^p(B/\varepsilon)^{L_n}(K/\varepsilon)^s$. By Theorem 2.5.6 in van der Vaart and Wellner (1996), we can conclude that the class $\{\ell(\boldsymbol{\theta}_n) : \boldsymbol{\theta}_n \in \mathcal{D} \times \mathcal{M}_B \times \mathcal{F}_B\}$ is Donsker and thus Glivenko-Cantelli.

Lemma 2. *Under conditions (C1)–(C3), we have*

$$\mathbb{M}(\boldsymbol{\theta}_0) - \mathbb{M}(\boldsymbol{\theta}) \asymp d^2(\boldsymbol{\theta}, \boldsymbol{\theta}_0),$$

for all $\boldsymbol{\theta}$ in the set $\{\boldsymbol{\theta} \in \mathcal{D} \times \mathcal{M}_B \times \mathcal{F}_B : d(\boldsymbol{\theta}, \boldsymbol{\theta}_0) < \delta\}$, where $\delta > 0$ is sufficiently small.

Proof. We first have

$$\begin{aligned} \mathbb{M}(\boldsymbol{\theta}_0) - \mathbb{M}(\boldsymbol{\theta}) &= E \left([1 - \exp\{-\mathcal{Y}(\mathbf{X}, \mathbf{U}; \boldsymbol{\theta})\}] m \left[\frac{1 - \exp\{-\mathcal{Y}_0(\mathbf{X}, \mathbf{U})\}}{1 - \exp\{-\mathcal{Y}(\mathbf{X}, \mathbf{U}; \boldsymbol{\theta})\}} \right] \right. \\ &\quad + [\exp\{-\mathcal{Y}(\mathbf{X}, \mathbf{V}; \boldsymbol{\theta})\} - \exp\{-\mathcal{Y}(\mathbf{X}, \mathbf{U}; \boldsymbol{\theta})\}] m \left[\frac{\exp\{-\mathcal{Y}_0(\mathbf{X}, \mathbf{V})\} - \exp\{-\mathcal{Y}_0(\mathbf{X}, \mathbf{U})\}}{\exp\{-\mathcal{Y}(\mathbf{X}, \mathbf{V}; \boldsymbol{\theta})\} - \exp\{-\mathcal{Y}(\mathbf{X}, \mathbf{U}; \boldsymbol{\theta})\}} \right] \\ &\quad \left. + \exp\{-\mathcal{Y}(\mathbf{X}, \mathbf{V}; \boldsymbol{\theta})\} m \left[\frac{\exp\{-\mathcal{Y}_0(\mathbf{X}, \mathbf{V})\}}{\exp\{-\mathcal{Y}(\mathbf{X}, \mathbf{V}; \boldsymbol{\theta})\}} \right] \right), \end{aligned}$$

where $m(x) = x \log x - x + 1$ and $(x-1)^2/4 \leq m(x) \leq (x-1)^2$ if $x \rightarrow 1$. Define $h(z) = 1 - \exp\{-\mathcal{Y}(\mathbf{X}, z; \boldsymbol{\theta})\}$, $h_0(z) = 1 - \exp\{-\mathcal{Y}_0(\mathbf{X}, z)\}$, and $\mathcal{G}(\mathbf{U}, \mathbf{V}; \boldsymbol{\theta}) = (\mathcal{Y}(\mathbf{X}, \mathbf{U}; \boldsymbol{\theta}) - \mathcal{Y}_0(\mathbf{X}, \mathbf{U}))^2 + (\mathcal{Y}(\mathbf{X}, \mathbf{V}; \boldsymbol{\theta}) - \mathcal{Y}_0(\mathbf{X}, \mathbf{V}))^2$. By Conditions (C1)–(C3), we utilize the Taylor series expansion and derive

$$\begin{aligned} \mathbb{M}(\boldsymbol{\theta}_0) - \mathbb{M}(\boldsymbol{\theta}) &= \\ &E \left\{ h(\mathbf{U}) m \left(\frac{h_0(\mathbf{U})}{h(\mathbf{U})} \right) + (h(\mathbf{U}) - h(\mathbf{V})) m \left(\frac{h_0(\mathbf{U}) - h_0(\mathbf{V})}{h(\mathbf{U}) - h(\mathbf{V})} \right) + (1 - h(\mathbf{V})) m \left(\frac{1 - h_0(\mathbf{V})}{1 - h(\mathbf{V})} \right) \right\} \\ &\gtrsim E \left\{ \frac{1}{h(\mathbf{U})} [h(\mathbf{U}) - h_0(\mathbf{U})]^2 + \frac{1}{1 - h(\mathbf{V})} [h(\mathbf{V}) - h_0(\mathbf{V})]^2 \right\} \\ &\gtrsim E \left\{ \frac{1}{\mathcal{Y}(\mathbf{X}, \mathbf{U}; \boldsymbol{\theta})} [\mathcal{Y}(\mathbf{X}, \mathbf{U}; \boldsymbol{\theta}) - \mathcal{Y}_0(\mathbf{X}, \mathbf{U})]^2 + \frac{1}{1 - \mathcal{Y}(\mathbf{X}, \mathbf{V}; \boldsymbol{\theta})} [\mathcal{Y}(\mathbf{X}, \mathbf{V}; \boldsymbol{\theta}) - \mathcal{Y}_0(\mathbf{X}, \mathbf{V})]^2 \right\} \\ &\gtrsim E \{\mathcal{G}(\mathbf{U}, \mathbf{V}; \boldsymbol{\theta})\}. \end{aligned}$$

Under Conditions (C1) and (C2), by Lemma 25.86 of van der Vaart (2000) and the mean value theorem, we have

$$\begin{aligned} E\{\Upsilon(\mathbf{X}, \mathbf{U}; \boldsymbol{\theta}) - \Upsilon_0(\mathbf{X}, \mathbf{U})\}^2 &\gtrsim E\{\|\boldsymbol{\beta} - \boldsymbol{\beta}_0\|^2 + \|\Lambda_\gamma(R) - \Lambda_0(R)\|_{L_2}^2 + \|\phi_\alpha(\mathbf{W}) - \phi_0(\mathbf{W})\|_{L_2}^2\} \\ &= d^2(\boldsymbol{\theta}, \boldsymbol{\theta}_0). \end{aligned}$$

Similarly, $E\{\Upsilon(\mathbf{X}, \mathbf{V}; \boldsymbol{\theta}) - \Upsilon_0(\mathbf{X}, \mathbf{V})\}^2 \gtrsim d^2(\boldsymbol{\theta}, \boldsymbol{\theta}_0)$. Then we have $E\{\mathcal{G}(\mathbf{U}, \mathbf{V}; \boldsymbol{\theta})\} \gtrsim d^2(\boldsymbol{\theta}, \boldsymbol{\theta}_0)$. By the inequality $m(x) \leq (x-1)^2$, we apply similar arguments as above to show that $\mathbb{M}(\boldsymbol{\theta}_0) - \mathbb{M}(\boldsymbol{\theta}) \lesssim E\{\mathcal{G}(\mathbf{U}, \mathbf{V}; \boldsymbol{\theta})\} \lesssim d^2(\boldsymbol{\theta}, \boldsymbol{\theta}_0)$. Thus, we have

$$\mathbb{M}(\boldsymbol{\theta}_0) - \mathbb{M}(\boldsymbol{\theta}) \asymp d^2(\boldsymbol{\theta}, \boldsymbol{\theta}_0).$$

Proof of Theorem 1. To establish the consistency of $\hat{\boldsymbol{\theta}}$, we proceed with the following three steps. First, since the class of functions $\{\ell(\boldsymbol{\theta}_n) : \boldsymbol{\theta}_n \in \mathcal{D} \times \mathcal{M}_B \times \mathcal{F}_B\}$ is shown to be Glivenko-Cantelli in Lemma 1, we have

$$\sup_{\boldsymbol{\theta}_n \in \mathcal{D} \times \mathcal{M}_B \times \mathcal{F}_B} |\mathbb{M}_n(\boldsymbol{\theta}_n) - \mathbb{M}(\boldsymbol{\theta}_n)| = o_p(1). \quad (\text{S3})$$

Second, we show that $\sup_{\boldsymbol{\theta}_n : d(\boldsymbol{\theta}_n, \boldsymbol{\theta}_0) \geq \delta} \mathbb{M}(\boldsymbol{\theta}_n) < \mathbb{M}(\boldsymbol{\theta}_0)$ for every $\delta > 0$, which is satisfied if we can prove the model identifiability. In particular, for any $\boldsymbol{\theta}_1$ and $\boldsymbol{\theta}_2 \in \mathcal{D} \times \mathcal{M}_B \times \mathcal{F}_B$, if $\ell(\boldsymbol{\theta}_1) = \ell(\boldsymbol{\theta}_2)$ with probability one, we need to show that $\boldsymbol{\theta}_1 = \boldsymbol{\theta}_2$. To this end, choosing $\delta_L = 1$ in $\ell(\boldsymbol{\theta}_1)$ and $\ell(\boldsymbol{\theta}_2)$, we obtain $\exp\{\boldsymbol{\beta}_1^\top \mathbf{X} + \phi_1(\mathbf{W})\} \Lambda_1(L) = \exp\{\boldsymbol{\beta}_2^\top \mathbf{X} + \phi_2(\mathbf{W})\} \Lambda_2(L)$. Thus, for any $t \in [a, b]$ and $\mathbf{W} \in \mathbb{R}^d$,

$$\exp\{\boldsymbol{\beta}_1^\top \mathbf{X} + \phi_1(\mathbf{W})\} \Lambda_1(t) = \exp\{\boldsymbol{\beta}_2^\top \mathbf{X} + \phi_2(\mathbf{W})\} \Lambda_2(t).$$

Taking the logarithm of both sides of the above equation leads to

$$\boldsymbol{\beta}_1^\top \mathbf{X} + \phi_1(\mathbf{W}) + \log\{\Lambda_1(t)\} = \boldsymbol{\beta}_2^\top \mathbf{X} + \phi_2(\mathbf{W}) + \log\{\Lambda_2(t)\}. \quad (\text{S4})$$

Further, taking expectation of both sides of the above equation with respect to \mathbf{W} and using the fact $E\{\phi_1(\mathbf{W})\} = E\{\phi_2(\mathbf{W})\} = 0$, we have

$$\beta_1^\top \mathbf{X} + \log\{\Lambda_1(t)\} = \beta_2^\top \mathbf{X} + \log\{\Lambda_2(t)\}.$$

By Condition (C8), we have $\beta_1 = \beta_2$ and $\Lambda_1(t) = \Lambda_2(t)$ for $t \in [a, b]$. By this conclusion and equation (S4), we have $\phi_1(\mathbf{W}) = \phi_2(\mathbf{W})$ for any $\mathbf{W} \in \mathbb{R}^d$. Thus, the proposed model is identifiable, and we have

$$\sup_{\theta_n: d(\theta_n, \theta_0) \geq \delta} \mathbb{M}(\theta_n) < \mathbb{M}(\theta_0). \quad (\text{S5})$$

Third, we show that $\mathbb{M}_n(\hat{\theta}) \geq \mathbb{M}_n(\theta_0) - o_p(1)$. Define $\mathcal{M}_{B/2} = \{\sum_{l=1}^{L_n} \gamma_l M_l(t) : 0 \leq \gamma_l \leq B/2, \text{ for } l = 1, \dots, L_n, t \in [a, b]\}$, $\mathcal{F}_{B/2} = \mathcal{F}(s, q, \mathbf{h}, B/2)$, $\Lambda_{0,n} = \arg \min_{\Lambda_\gamma \in \mathcal{M}_{B/2}} \|\Lambda_\gamma - \Lambda_0\|_{L_2}$ and $\phi_{0,n} = \arg \min_{\phi_\alpha \in \mathcal{F}_{B/2}} \|\phi_\alpha - \phi_0\|_{L_2}$. By Condition (C4), according to Corollary 6.21 of Schumaker (2007) and Lemma A1 of Lu et al. (2007), we have $\|\Lambda_{0,n} - \Lambda_0\|_{L_2} = O(n^{-\xi\nu})$, where $1/(2\xi + 1) < \nu < 1/(2\xi)$. Furthermore, according to Theorem 1 of Schmidt-Hieber (2020), we have $\|\phi_{0,n} - \phi_0\|_{L_2} = O(\alpha_n \log^2 n)$.

Define $\theta_{0,n} = (\beta_0, \Lambda_{0,n}, \phi_{0,n})$ and $\theta'_{0,n} = (\beta_0, \Lambda_0, \phi_{0,n})$. By (S3), Lemma 2 and the law of large numbers, we have

$$\begin{aligned} |\mathbb{M}_n(\theta_{0,n}) - \mathbb{M}_n(\theta_0)| &\leq |\mathbb{M}_n(\theta_{0,n}) - \mathbb{M}(\theta_{0,n})| + |\mathbb{M}(\theta_{0,n}) - \mathbb{M}(\theta'_{0,n})| \\ &\quad + |\mathbb{M}(\theta'_{0,n}) - \mathbb{M}(\theta_0)| + |\mathbb{M}(\theta_0) - \mathbb{M}_n(\theta_0)| \\ &= o_p(1). \end{aligned}$$

Then, we can obtain

$$\mathbb{M}_n(\hat{\theta}) - \mathbb{M}_n(\theta_0) \geq \mathbb{M}_n(\theta_{0,n}) - \mathbb{M}_n(\theta_0) \geq -o_p(1),$$

which gives

$$\mathbb{M}_n(\hat{\theta}) \geq \mathbb{M}_n(\theta_0) - o_p(1). \quad (\text{S6})$$

Based on the uniform convergence of \mathbb{M}_n to \mathbb{M} as obtained from (S3), we have $\mathbb{M}_n(\boldsymbol{\theta}_0) \xrightarrow{p} \mathbb{M}(\boldsymbol{\theta}_0)$ and $\mathbb{M}_n(\hat{\boldsymbol{\theta}}) \geq \mathbb{M}(\boldsymbol{\theta}_0) - o_p(1)$. The latter implies

$$\begin{aligned} \mathbb{M}(\boldsymbol{\theta}_0) - \mathbb{M}(\hat{\boldsymbol{\theta}}) &\leq \mathbb{M}_n(\hat{\boldsymbol{\theta}}) - \mathbb{M}(\hat{\boldsymbol{\theta}}) + o_p(1) \\ &\leq \sup_{\boldsymbol{\theta}_n \in \mathcal{D} \times \mathcal{M}_B \times \mathcal{F}_B} |\mathbb{M}_n(\boldsymbol{\theta}_n) - \mathbb{M}(\boldsymbol{\theta}_n)| + o_p(1) \xrightarrow{p} 0 \end{aligned}$$

According to the inequality (S5), for every $\delta > 0$, there exists a positive number $c_\theta > 0$ such that $\mathbb{M}(\boldsymbol{\theta}) < \mathbb{M}(\boldsymbol{\theta}_0) - c_\theta$ for any $\boldsymbol{\theta}$ with $d(\boldsymbol{\theta}, \boldsymbol{\theta}_0) \geq \delta$. Clearly, the event $\{d(\hat{\boldsymbol{\theta}}, \boldsymbol{\theta}_0) \geq \delta\}$ is contained in the event $\{\mathbb{M}(\hat{\boldsymbol{\theta}}) < \mathbb{M}(\boldsymbol{\theta}_0) - c_\theta\}$, and the probability of the event $\{\mathbb{M}(\hat{\boldsymbol{\theta}}) < \mathbb{M}(\boldsymbol{\theta}_0) - c_\theta\}$ converges to 0. Hence, we have $d(\hat{\boldsymbol{\theta}}, \boldsymbol{\theta}_0) = o_p(1)$.

Proof of Theorem 2. For $\delta > 0$, define $\Theta_\delta = \{\boldsymbol{\theta}_n \in \mathcal{D} \times \mathcal{M}_B \times \mathcal{F}_B, \delta/2 \leq d(\boldsymbol{\theta}_n, \boldsymbol{\theta}_0) \leq \delta\}$.

From Lemma 2, we have $\mathbb{M}(\boldsymbol{\theta}_0) - \mathbb{M}(\boldsymbol{\theta}) \gtrsim d^2(\boldsymbol{\theta}, \boldsymbol{\theta}_0) \gtrsim \delta^2$, leading to

$$\sup_{\boldsymbol{\theta}_n \in \Theta_\delta} [\mathbb{M}(\boldsymbol{\theta}_n) - \mathbb{M}(\boldsymbol{\theta}_0)] \lesssim -\delta^2.$$

Recall that $\boldsymbol{\theta}_{0,n} = (\boldsymbol{\beta}_0, \Lambda_{0,n}, \phi_{0,n})$, where $\Lambda_{0,n} = \arg \min_{\Lambda_\gamma \in \mathcal{M}_{B/2}} \|\Lambda_\gamma - \Lambda_0\|_{L_2}$ and $\phi_{0,n} = \arg \min_{\phi_\alpha \in \mathcal{F}_{B/2}} \|\phi_\alpha - \phi_0\|_{L_2}$. Let $\mathcal{L}_\delta = \{\ell(\boldsymbol{\theta}_n) - \ell(\boldsymbol{\theta}_{0,n}) : \boldsymbol{\theta}_n \in \mathcal{D} \times \mathcal{M}_B \times \mathcal{F}_B, d(\boldsymbol{\theta}_n, \boldsymbol{\theta}_{0,n}) \leq \delta\}$. We have

$$\|\mathbb{G}_n\|_{\mathcal{L}_\delta} = \sup_{\substack{\boldsymbol{\theta}_n \in \mathcal{D} \times \mathcal{M}_B \times \mathcal{F}_B, \\ d(\boldsymbol{\theta}_n, \boldsymbol{\theta}_{0,n}) \leq \delta}} |\mathbb{G}_n \ell(\boldsymbol{\theta}_n) - \mathbb{G}_n \ell(\boldsymbol{\theta}_{0,n})|.$$

By Condition (C1) and Theorem 9.23 of Kosorok (2008), for any $\delta > 0$ and $0 < \varepsilon < \delta$, the ε -bracketing number of $\{\boldsymbol{\beta} \in \mathcal{D} : \|\boldsymbol{\beta} - \boldsymbol{\beta}_0\| \leq \delta\}$ with radius ε and Euclidean norm is bounded by $M(\delta/\varepsilon)^p$. By Condition(C4), following the proof of Lemma 1 and the calculations of Shen and Wong (1994) (pp. 597), we conclude that the logarithms of the ε -bracketing numbers of $\mathcal{M}_\delta = \{\Lambda_\gamma \in \mathcal{M}_B : \|\Lambda_\gamma - \Lambda_{0,n}\|_{L_2} \leq \delta\}$ and $\mathcal{F}_\delta = \{\phi_\alpha \in \mathcal{F}_B : \|\phi_\alpha - \phi_{0,n}\|_{L_2} \leq \delta\}$ equipped with $L_2(\mathbb{P})$ are bounded by $ML_n \log(\delta/\varepsilon)$ and $Ms \log(K/\varepsilon)$, respectively. Therefore, it follows that if $p \leq s$ and $\delta \leq K$,

$$\log N_{[]}(\varepsilon, \mathcal{L}_\delta, L_2(\mathbb{P})) \lesssim p \log(\delta/\varepsilon) + L_n \log(\delta/\varepsilon) + s \log(K/\varepsilon) \lesssim (s + L_n) \log(K/\varepsilon).$$

Define the entropy integral $J_{\square}(\delta, \mathcal{F}, L_2(\mathbb{P}))$ as $\int_0^\delta \sqrt{1 + \log N_{\square}(\varepsilon, \mathcal{F}, L_2(\mathbb{P}))} d\varepsilon$. We obtain

$$\begin{aligned} J_{\square}(\delta, \mathcal{L}_\delta, L_2(\mathbb{P})) &\lesssim \int_0^\delta \sqrt{1 + (s + L_n) \log(K/\varepsilon)} d\varepsilon \\ &= \frac{2K}{(s + L_n)} e^{1/(s+L_n)} \int_{\sqrt{1+(s+L_n)\log(K/\delta)}}^\infty u^2 \exp^{-u^2/(s+L_n)} du \\ &\asymp \delta \sqrt{(s + L_n) \log K/\delta}. \end{aligned}$$

The second equality holds by setting $u = \sqrt{1 + (s + L_n) \log(K/\varepsilon)}$. The last inequality holds due to the fact that $u > \sqrt{(s + L_n) \log(K/\varepsilon)}$. Referring to the Lemma 3.4.3 in van der Vaart and Wellner (1996), we have

$$\begin{aligned} \mathbb{E}^* \|\mathbb{G}_n\|_{\mathcal{L}_\delta} &\lesssim J_{\square}(\delta, \mathcal{L}_\delta, L_2(\mathbb{P})) \left\{ 1 + \frac{J_{\square}(\delta, \mathcal{L}_\delta, L_2(\mathbb{P}))}{\delta^2 \sqrt{n}} \right\} \\ &\lesssim \delta \sqrt{(s + L_n) \log(K/\delta)} + \frac{(s + L_n)}{\sqrt{n}} \log(K/\delta). \end{aligned}$$

To derive the convergence rate of the proposed estimator, we let the pivotal function $\phi_n(\delta)$ defined in Theorem 3.2.5 of van der Vaart and Wellner (1996) take the form $\phi_n(\delta) = \delta \sqrt{(s + L_n) \log(K/\delta)} + \frac{(s+L_n)}{\sqrt{n}} \log(K/\delta)$. Based on the preceding results $\|\phi_{0,n} - \phi_0\|_{L_2} = O(\alpha_n \log^2 n)$ and $\|\Lambda_{0,n} - \Lambda_0\|_{L_2} = O(n^{-\xi\nu})$, we obtain

$$\mathbb{E}^* \sup_{\boldsymbol{\theta}_n \in \Theta_\delta} \sqrt{n} |(\mathbb{M}_n - \mathbb{M})(\boldsymbol{\theta}_n) - (\mathbb{M}_n - \mathbb{M})(\boldsymbol{\theta}_0)| \lesssim \phi_n(\delta).$$

We set r_n defined in Theorem 3.2.5 of van der Vaart and Wellner (1996) to $r_n = (\alpha_n \log^2 n + n^{-\xi\nu})^{-1}$. By Condition (C2), Condition (C6) and $p_n = O(n^\nu)$, we have

$$r_n^2 \phi_n(1/r_n) = \frac{\frac{1}{r_n} \sqrt{(s + L_n) \log(Kr_n)} + \frac{(s+L_n)}{\sqrt{n}} \log(Kr_n)}{(\alpha_n \log^2 n + n^{-\xi\nu})^2} \leq \sqrt{n}.$$

Therefore, we can choose $r_n = (\alpha_n \log^2 n + n^{-\xi\nu})^{-1}$ such that

$$\begin{aligned} |\mathbb{M}_n(\boldsymbol{\theta}_{0,n}) - \mathbb{M}_n(\boldsymbol{\theta}_0)| &\lesssim |(\mathbb{M}_n - \mathbb{M})(\boldsymbol{\theta}_{0,n}) - (\mathbb{M}_n - \mathbb{M})(\boldsymbol{\theta}_0)| + |\mathbb{M}(\boldsymbol{\theta}_{0,n}) - \mathbb{M}(\boldsymbol{\theta}_0)| \\ &\lesssim O_p(\phi_n(1/r_n)/\sqrt{n}) + \|\phi_{0,n} - \phi_0\|_{L_2}^2 + \|\Lambda_{0,n} - \Lambda_0\|_{L_2}^2 \\ &= O_p(r_n^{-2}). \end{aligned}$$

By the definition of $\hat{\boldsymbol{\theta}}$, we derive the inequalities

$$\mathbb{M}_n(\hat{\boldsymbol{\theta}}) - \mathbb{M}_n(\boldsymbol{\theta}_0) \geq \mathbb{M}_n(\boldsymbol{\theta}_{0,n}) - \mathbb{M}_n(\boldsymbol{\theta}_0) \geq -O_p(r_n^{-2}),$$

According to Theorem 3.2.5 from van der Vaart and Wellner (1996), it follows that $r_n d(\hat{\boldsymbol{\theta}}, \boldsymbol{\theta}_0) = O_p(1)$. In other words, $d(\hat{\boldsymbol{\theta}}, \boldsymbol{\theta}_0) = O_p(\alpha_n \log^2 n + n^{-\xi\nu})$.

Proof of Theorem 3. Define

$$\begin{aligned} Q_1(\mathbf{X}, \mathbf{U}, \mathbf{V}; \boldsymbol{\theta}) &= \delta_L \left(\frac{\exp\{-\mathcal{Y}(\mathbf{X}, \mathbf{U}; \boldsymbol{\theta})\} G'[\exp\{\boldsymbol{\beta}^\top \mathbf{X} + \psi(\mathbf{U})\}] \exp\{\boldsymbol{\beta}^\top \mathbf{X} + \psi(\mathbf{U})\}}{1 - \exp\{-\mathcal{Y}(\mathbf{X}, \mathbf{U}; \boldsymbol{\theta})\}} \right) \\ &\quad + \delta_I \left(\frac{\exp\{-\mathcal{Y}(\mathbf{X}, \mathbf{U}; \boldsymbol{\theta})\} G'[\exp\{\boldsymbol{\beta}^\top \mathbf{X} + \psi(\mathbf{U})\}] \exp\{\boldsymbol{\beta}^\top \mathbf{X} + \psi(\mathbf{U})\}}{\exp\{-\mathcal{Y}(\mathbf{X}, \mathbf{V}; \boldsymbol{\theta})\} - \exp\{-\mathcal{Y}(\mathbf{X}, \mathbf{U}; \boldsymbol{\theta})\}} \right), \\ Q_2(\mathbf{X}, \mathbf{U}, \mathbf{V}; \boldsymbol{\theta}) &= -\delta_I \left(\frac{\exp\{-\mathcal{Y}(\mathbf{X}, \mathbf{V}; \boldsymbol{\theta})\} G'[\exp\{\boldsymbol{\beta}^\top \mathbf{X} + \psi(\mathbf{V})\}] \exp\{\boldsymbol{\beta}^\top \mathbf{X} + \psi(\mathbf{V})\}}{\exp\{-\mathcal{Y}(\mathbf{X}, \mathbf{V}; \boldsymbol{\theta})\} - \exp\{-\mathcal{Y}(\mathbf{X}, \mathbf{U}; \boldsymbol{\theta})\}} \right) \\ &\quad - \delta_R (G'[\exp\{\boldsymbol{\beta}^\top \mathbf{X} + \psi(\mathbf{V})\}] \exp\{\boldsymbol{\beta}^\top \mathbf{X} + \psi(\mathbf{V})\}). \end{aligned}$$

The score function for $\boldsymbol{\beta}$ is

$$\dot{\ell}_{\boldsymbol{\beta}}(\boldsymbol{\theta}_0) = \left. \frac{\partial \ell(\boldsymbol{\beta}, \Lambda_0, \phi_0)}{\partial \boldsymbol{\beta}} \right|_{\boldsymbol{\beta}=\boldsymbol{\beta}_0} = \mathbf{X}(Q_1(\mathbf{X}, \mathbf{U}, \mathbf{V}; \boldsymbol{\theta}_0) + Q_2(\mathbf{X}, \mathbf{U}, \mathbf{V}; \boldsymbol{\theta}_0)).$$

Consider any parametric submodel of Λ denoted as $\Lambda_{\kappa, q}(t) = \Lambda(t) + \kappa q(t)$, where $q \in L_2([a, b])$. The score function along this submodel is

$$\dot{\ell}_{\Lambda}(\boldsymbol{\theta}_0)[q] = \left. \frac{\partial \ell(\boldsymbol{\beta}_0, \Lambda_{\kappa, q}, \phi_0)}{\partial \kappa} \right|_{\kappa=0} = \frac{q(R)}{\Lambda(R)} Q_1(\mathbf{X}, \mathbf{U}, \mathbf{V}; \boldsymbol{\theta}_0) + \frac{q(L)}{\Lambda(L)} Q_2(\mathbf{X}, \mathbf{U}, \mathbf{V}; \boldsymbol{\theta}_0).$$

To derive the score operator for ϕ , we consider any parametric submodel of ϕ given by $\phi_{\zeta, z}(\mathbf{w}) = \phi(\mathbf{w}) + \zeta z(\mathbf{w})$, where $z \in L_2([e, f]^d)$. The score function along this submodel is

$$\dot{\ell}_{\phi}(\boldsymbol{\theta}_0)[z] = \left. \frac{\partial \ell(\boldsymbol{\beta}_0, \Lambda_0, \phi_{\zeta, z})}{\partial \zeta} \right|_{\zeta=0} = z(\mathbf{w})(Q_1(\mathbf{X}, \mathbf{U}, \mathbf{V}; \boldsymbol{\theta}_0) + Q_2(\mathbf{X}, \mathbf{U}, \mathbf{V}; \boldsymbol{\theta}_0)).$$

Let Ψ_{Λ_0} be the collection of all subfamilies $\{\Lambda_{\kappa, q} : \kappa \in (-1, 1)\} \subset \{\Lambda : \Lambda \in \bar{\Psi}_{\Lambda}\}$ such that $\lim_{\kappa \rightarrow 0} \|\kappa^{-1}(\Lambda_{\kappa, q} - \Lambda_0) - q\|_{L_2} = 0$, where $q \in L_2([a, b])$, and let

$$\begin{aligned} \Omega_{\Lambda_0} &= \{q \in L_2([a, b]) : \lim_{\kappa \rightarrow 0} \|\kappa^{-1}(\Lambda_{\kappa, q} - \Lambda_0) - q\|_{L_2} = 0 \text{ for some subfamily} \\ &\quad \{\Lambda_{\kappa, q} : \kappa \in (-1, 1)\} \in \Psi_{\Lambda_0}\}. \end{aligned}$$

Similarly, let Ψ_{ϕ_0} denote the collection of all subfamilies $\{\phi_{\zeta, z} \in L_2([e, f]^d) : \zeta \in (-1, 1)\} \subset \bar{\Psi}_{\phi}$ such that $\lim_{\zeta \rightarrow 0} \|\zeta^{-1}(\phi_{\zeta, z} - \phi_0) - z\|_{L_2} = 0$, where $z \in L_2([e, f]^d)$, and let

$$\begin{aligned} \Omega_{\phi_0} &= \{z \in L_2([e, f]^d) : \lim_{\zeta \rightarrow 0} \|\zeta^{-1}(\phi_{\zeta, z} - \phi_0) - z\|_{L_2} = 0 \text{ for some subfamily} \\ &\quad \{\phi_{\zeta, z} : \zeta \in (-1, 1)\} \in \Psi_{\phi_0}, \text{ and } E\{z(\mathbf{W})\} = 0\}. \end{aligned}$$

Let $\overline{\Omega}_{\Lambda_0}$ and $\overline{\Omega}_{\phi_0}$ be the closed linear span of Ω_{Λ_0} and Ω_{ϕ_0} , respectively. Define $\dot{\ell}_\phi(\boldsymbol{\theta}_0)[\mathbf{z}] = (\dot{\ell}_\phi(\boldsymbol{\theta}_0)[z_1], \dots, \dot{\ell}_\phi(\boldsymbol{\theta}_0)[z_p])^\top$ and $\dot{\ell}_\Lambda(\boldsymbol{\theta}_0)[\mathbf{q}] = (\dot{\ell}_\Lambda(\boldsymbol{\theta}_0)[q_1], \dots, \dot{\ell}_\Lambda(\boldsymbol{\theta}_0)[q_p])^\top$, where $\mathbf{z} = (z_1, \dots, z_p)^\top \in \overline{\Omega}_{\phi_0}^p$, $\mathbf{q} = (q_1, \dots, q_p)^\top \in \overline{\Omega}_{\Lambda_0}^p$.

Referring to Theorem 1 in Bickel et al. (1993)(pp. 70), under Conditions (C1)–(C3) and (C7), the efficient score vector for $\boldsymbol{\beta}$ is defined as

$$\ell_\beta^*(\boldsymbol{\theta}_0) = \dot{\ell}_\beta(\boldsymbol{\theta}_0) - \dot{\ell}_\Lambda(\boldsymbol{\theta}_0)[\mathbf{q}^*] - \dot{\ell}_\phi(\boldsymbol{\theta}_0)[\mathbf{z}^*],$$

where $(\mathbf{q}^{*\top}, \mathbf{z}^{*\top})^\top \in \overline{\Omega}_{\Lambda_0}^p \times \overline{\Omega}_{\phi_0}^p$ represents the least favorable direction chosen such that $\ell_\beta^*(\boldsymbol{\theta}_0)$ is orthogonal to $\dot{\ell}_\Lambda(\boldsymbol{\theta}_0)[\mathbf{q}^*]$ and $\dot{\ell}_\phi(\boldsymbol{\theta}_0)[\mathbf{z}^*]$, respectively. This involves solving the following normal equations to obtain \mathbf{q}^* and \mathbf{z}^* :

$$\dot{\ell}_\beta(\boldsymbol{\theta}_0)\dot{\ell}_\Lambda^*(\boldsymbol{\theta}_0) = (\dot{\ell}_\Lambda(\boldsymbol{\theta}_0)[\mathbf{q}^*] + \dot{\ell}_\phi(\boldsymbol{\theta}_0)[\mathbf{z}^*])\dot{\ell}_\Lambda^*(\boldsymbol{\theta}_0),$$

and

$$\dot{\ell}_\beta(\boldsymbol{\theta}_0)\dot{\ell}_\phi^*(\boldsymbol{\theta}_0) = (\dot{\ell}_\Lambda(\boldsymbol{\theta}_0)[\mathbf{q}^*] + \dot{\ell}_\phi(\boldsymbol{\theta}_0)[\mathbf{z}^*])\dot{\ell}_\phi^*(\boldsymbol{\theta}_0),$$

where $\dot{\ell}_\Lambda^*(\boldsymbol{\theta}_0)$ and $\dot{\ell}_\phi^*(\boldsymbol{\theta}_0)$ denote the adjoint operator of $\dot{\ell}_\Lambda(\boldsymbol{\theta}_0)$ and $\dot{\ell}_\phi(\boldsymbol{\theta}_0)$, respectively. To prove the asymptotic normality of $\hat{\boldsymbol{\beta}}$, we need to verify the following three conditions:

- (1) \mathbf{z}^* and \mathbf{q}^* exist, which ensures the existence of the efficient score $\ell_\beta^*(\hat{\boldsymbol{\theta}})$;
- (2) the efficient score $\ell_\beta^*(\hat{\boldsymbol{\theta}})$ belongs to a Donsker class and converges to $\ell_\beta^*(\boldsymbol{\theta}_0) = \dot{\ell}_\beta(\boldsymbol{\theta}_0) - \dot{\ell}_\Lambda(\boldsymbol{\theta}_0)[\mathbf{q}^*] - \dot{\ell}_\phi(\boldsymbol{\theta}_0)[\mathbf{z}^*]$ in the $L_2(\mathbb{P})$ -norm;
- (3) the matrix $\mathbf{I}(\boldsymbol{\beta}_0) = E\{\ell_\beta^*(\boldsymbol{\theta}_0)\ell_\beta^*(\boldsymbol{\theta}_0)^\top\}$ is nonsingular.

For Condition (1), the existence of \mathbf{z}^* and \mathbf{q}^* can be established through same arguments as presented in Theorem 6.1 of Huang and Rossini (1997). Next, we verify Condition (2). Similar to the proof of Theorem 2, for every $\delta > 0$, we can conclude that the class $\{\dot{\ell}_\beta(\boldsymbol{\theta}_n) : \boldsymbol{\theta}_n \in \mathcal{D} \times \mathcal{M}_B \times \mathcal{F}_B, d(\boldsymbol{\theta}_n, \boldsymbol{\theta}_0) \leq \delta\}$ has bounded ε -bracketing number $M(\delta/\varepsilon)^p$ and is thus Donsker. Similar arguments show that $\{\dot{\ell}_\Lambda(\boldsymbol{\theta}_n)[\mathbf{q}^*] : \boldsymbol{\theta}_n \in \mathcal{D} \times \mathcal{M}_B \times \mathcal{F}_B, d(\boldsymbol{\theta}_n, \boldsymbol{\theta}_0) \leq \delta\}$

and $\{\dot{\ell}_\phi(\boldsymbol{\theta}_n)[\mathbf{z}^*] : \boldsymbol{\theta}_n \in \mathcal{D} \times \mathcal{M}_B \times \mathcal{F}_B, d(\boldsymbol{\theta}_n, \boldsymbol{\theta}_0) \leq \delta\}$ are both Donsker class. It then follows from the preservation of the Donsker property that $\ell_\beta^*(\hat{\boldsymbol{\theta}})$ belongs to a Donsker class. Based on Theorem 1, we can conclude that $\ell_\beta^*(\hat{\boldsymbol{\theta}})$ converges to $\ell_\beta^*(\boldsymbol{\theta}_0)$ in $L_2(\mathbb{P})$ -norm, implying that $\mathbb{G}_n\{\ell_\beta^*(\hat{\boldsymbol{\theta}})\}$ converges in distribution to a zero-mean p -variate normal random vector. By the definition of $\hat{\boldsymbol{\theta}}$, we have $\mathbb{P}_n\{\ell_\beta^*(\hat{\boldsymbol{\theta}})\} = 0$, it follows that

$$\mathbb{G}_n\{\ell_\beta^*(\hat{\boldsymbol{\theta}})\} = -n^{1/2}\mathbb{P}\{\ell_\beta^*(\hat{\boldsymbol{\theta}}) - \ell_\beta^*(\boldsymbol{\theta}_0)\}.$$

By the Taylor series expansion, we have

$$\mathbb{G}_n\{\ell_\beta^*(\hat{\boldsymbol{\theta}})\} = n^{1/2}\mathbf{I}(\boldsymbol{\beta}_0)(\hat{\boldsymbol{\beta}} - \boldsymbol{\beta}_0) + O(n^{1/2}d^2(\hat{\boldsymbol{\theta}}, \boldsymbol{\theta}_0)). \quad (\text{S7})$$

By the convergence rate $d(\hat{\boldsymbol{\theta}}, \boldsymbol{\theta}_0) = O_p(\alpha_n \log^2 n + n^{-\xi\nu})$ and assuming $(2\xi + 1)^{-1} < \nu < (2\xi)^{-1}$ with $\xi \geq 1$ and $\sqrt{n}\alpha_n^2 \rightarrow 0$ as $n \rightarrow \infty$, it follows that $d^2(\hat{\boldsymbol{\theta}}, \boldsymbol{\theta}_0) = o_p(n^{-1/2})$.

Finally, we show that $\mathbf{I}(\boldsymbol{\beta}_0)$ is nonsingular. Suppose that the matrix $\mathbf{I}(\boldsymbol{\beta}_0)$ is singular, there exists a nonzero vector $\tilde{\boldsymbol{\eta}}$ such that

$$\tilde{\boldsymbol{\eta}}^\top \mathbf{I}(\boldsymbol{\beta}_0) \tilde{\boldsymbol{\eta}} = \tilde{\boldsymbol{\eta}}^\top E\{\ell_\beta^*(\boldsymbol{\theta}_0) \ell_\beta^*(\boldsymbol{\theta}_0)^\top\} \tilde{\boldsymbol{\eta}} = 0.$$

This indicates that the score function along the submodel $\{\boldsymbol{\beta}_0 + \kappa \tilde{\boldsymbol{\eta}}, \Lambda_0 + \kappa \tilde{\boldsymbol{\eta}}^\top \mathbf{q}^*, \phi_0 + \kappa \tilde{\boldsymbol{\eta}}^\top \mathbf{z}^*\}$ is zero with probability 1, that is

$$\begin{aligned} & Q_1(\mathbf{X}, \mathbf{U}, \mathbf{V}; \boldsymbol{\theta}_0)[\tilde{\boldsymbol{\eta}}^\top \mathbf{X} + \tilde{\boldsymbol{\eta}}^\top \mathbf{z}^*(w) + \tilde{\boldsymbol{\eta}}^\top \mathbf{q}^*(R)/\Lambda_0(R)] \\ & + Q_2(\mathbf{X}, \mathbf{U}, \mathbf{V}; \boldsymbol{\theta}_0)[\tilde{\boldsymbol{\eta}}^\top \mathbf{X} + \tilde{\boldsymbol{\eta}}^\top \mathbf{z}^*(w) + \tilde{\boldsymbol{\eta}}^\top \mathbf{q}^*(L)/\Lambda_0(L)] = 0. \end{aligned}$$

We consider $\delta_L = 1$, and then have $Q_1(\mathbf{X}, \mathbf{U}, \mathbf{V}; \boldsymbol{\theta}_0)[\tilde{\boldsymbol{\eta}}^\top \mathbf{X} + \tilde{\boldsymbol{\eta}}^\top \mathbf{z}^*(w) + \tilde{\boldsymbol{\eta}}^\top \mathbf{q}^*(R)/\Lambda_0(R)] = 0$

Therefore, with probability 1, $\tilde{\boldsymbol{\eta}}^\top \mathbf{X} + \tilde{\boldsymbol{\eta}}^\top \mathbf{q}^*(R)/\Lambda_0(R) + \tilde{\boldsymbol{\eta}}^\top \mathbf{z}^*(w) = 0$. It then follows that $\tilde{\boldsymbol{\eta}} = 0$ by Condition (C8). This contradicts the fact that $\tilde{\boldsymbol{\eta}}$ is a nonzero vector. Therefore, $\mathbf{I}(\boldsymbol{\beta}_0)$ is nonsingular. By (S7), we have

$$\sqrt{n}(\hat{\boldsymbol{\beta}} - \boldsymbol{\beta}_0) \xrightarrow{d} N(\mathbf{0}, \mathbf{I}^{-1}(\boldsymbol{\beta}_0)), n \rightarrow \infty,$$

which completes the proof of Theorem 3.

Section S.3: Additional simulation results

In this section, we conducted simulations under the PO model. In particular, the failure times of interest were generated from model (1) with $G(x) = \log(1 + x)$. Other simulation configurations remained the same as the simulation study of the main manuscript. The results summarized in Tables S1 and S2 suggest similar conclusions as Section 4 of the main manuscript regarding the comparisons of the proposed method, “Spline-Trans” and “NPMLE-Trans”. In addition, it is worth pointing out that the performances of “deep PH” and “penalized PH” deteriorate remarkably here due to using a misspecified PH model.

Section S.4: More details about ADNI data and prediction evaluation

In the ADNI data analysis, we focused on 14 potential risk factors for AD, consisting of a genetic covariate: `APOE ϵ 4` (coded as 0, 1, or 2 based on the number of APOE 4 alleles), four demographic covariates: `Age` (given in years), `Gender` (1 for male and 0 for female), `Education` (years of education), `Marry` (for married and 0 otherwise), and nine test scores characterizing cognitive ability, memory and executive function: `ADAS11` (a test score measured by the AD Assessment Scale Cognitive Subscales (ADAS) 11), `ADAS13` (a test score measured by the ADAS13), `MMSE` (a test score measured by the Mini-Mental State Examination), `RAVLT.i` (the immediate recall in the Rey Auditory Verbal Learning Test (RAVLT)), `RAVLT.l` (learning ability in the RAVLT), `RAVLT.d` (30-minute delayed recall in the RAVLT), `DelayRec` (30-minute delayed recognition in the RAVLT), `TrailA` (a score obtained from the Trail Making Test Part A), and `TrailB` (a score obtained from the Trail Making Test Part B). In particular, `ADAS11`, `ADAS13`, and `MMSE` collectively assess an individual’s cognitive ability. An individual with higher `ADAS11` and `ADAS13` has a worse

Table S1: Simulation results for the regression parameter estimates under the PO model. Results include the estimation bias (Bias), the sample standard error (SSE) of the estimates, the average of the standard error estimates (SEE), and the 95% coverage probability (CP95).

Case	n	par.	Proposed method				Deep PH		Spline-Trans		Penalized PH		NPMLE-Trans	
			Bias	SSE	SEE	CP95	Bias	SSE	Bias	SSE	Bias	SSE	Bias	SSE
1	500	β_1	0.006	0.117	0.126	0.970	-0.086	0.123	0.038	0.136	-0.138	0.097	0.014	0.120
		β_2	-0.003	0.234	0.239	0.950	0.109	0.252	-0.038	0.253	0.232	0.233	-0.011	0.237
	1000	β_1	0.018	0.084	0.087	0.955	-0.093	0.104	0.035	0.090	-0.110	0.066	0.030	0.086
		β_2	-0.019	0.171	0.166	0.945	0.094	0.184	-0.037	0.181	0.147	0.167	-0.033	0.174
2	500	β_1	-0.022	0.111	0.126	0.985	-0.113	0.133	0.037	0.127	-0.171	0.098	-0.036	0.110
		β_2	0.015	0.232	0.238	0.975	0.111	0.248	-0.037	0.255	0.262	0.235	0.030	0.237
	1000	β_1	-0.004	0.089	0.087	0.960	-0.109	0.109	0.034	0.093	-0.145	0.070	-0.018	0.090
		β_2	0.005	0.170	0.164	0.945	0.077	0.198	-0.036	0.179	0.190	0.169	0.021	0.170
3	500	β_1	0.003	0.119	0.125	0.980	-0.081	0.138	0.033	0.133	-0.141	0.095	-0.003	0.118
		β_2	0.008	0.238	0.237	0.965	0.082	0.286	-0.032	0.265	0.234	0.233	0.012	0.241
	1000	β_1	0.010	0.088	0.086	0.955	-0.087	0.107	0.020	0.092	-0.116	0.069	0.009	0.089
		β_2	-0.006	0.168	0.163	0.940	0.074	0.185	-0.022	0.178	0.157	0.162	-0.009	0.170
4	500	β_1	0.033	0.128	0.120	0.924	-0.113	0.121	0.114	0.154	-0.147	0.104	0.023	0.123
		β_2	-0.009	0.207	0.222	0.965	0.060	0.249	-0.086	0.258	0.248	0.201	0.001	0.204
	1000	β_1	<0.001	0.079	0.081	0.945	-0.124	0.091	0.033	0.087	-0.157	0.058	-0.006	0.078
		β_2	0.002	0.159	0.151	0.955	0.087	0.178	-0.031	0.174	0.194	0.139	0.009	0.155
5	500	β_1	-0.001	0.128	0.129	0.945	-0.163	0.145	0.115	0.167	-0.184	0.109	-0.024	0.122
		β_2	0.015	0.231	0.233	0.955	0.131	0.250	-0.099	0.309	0.281	0.223	0.039	0.227
	1000	β_1	-0.022	0.089	0.086	0.940	-0.194	0.100	0.038	0.098	-0.189	0.066	-0.048	0.083
		β_2	0.035	0.165	0.155	0.930	0.169	0.178	-0.029	0.195	0.249	0.157	0.059	0.155
6	500	β_1	-0.002	0.133	0.125	0.919	-0.168	0.114	0.067	0.161	-0.198	0.103	-0.048	0.123
		β_2	0.016	0.224	0.225	0.929	0.124	0.246	-0.050	0.269	0.276	0.197	0.057	0.214
	1000	β_1	-0.029	0.079	0.083	0.954	-0.164	0.094	-0.019	0.085	-0.210	0.054	-0.082	0.076
		β_2	0.039	0.154	0.147	0.929	0.096	0.197	0.010	0.173	0.251	0.144	0.086	0.147

* Note: "Proposed method" denotes the proposed deep regression approach, "Deep PH" refers to the deep learning approach for the partially linear PH model (Du et al., 2024), "Spline-Trans" refers to the sieve MLE approach for the partially linear additive transformation model (Yuan et al., 2024), "Penalized PH" refers to penalized MLE method for the PH model with linear covariate effects (Zhao et al., 2020), "NPMLE-Trans" refers to the nonparametric MLE method for the transformation model with linear covariate effects (Zeng et al., 2016).

Table S2: Simulation results for the relative error (RE) of $\hat{\phi}_{\alpha}$ over ϕ and the mean squared error (MSE) of the estimated survival function. Values of MSE in the table are multiplied by 100.

Case	n	Proposed method		Deep PH		Spline-Trans		Penalized PH		NPMLE-Trans	
		RE	MSE	RE	MSE	RE	MSE	RE	MSE	RE	MSE
1	500	0.399	0.268	0.565	0.829	2.285	0.819	0.435	0.378	0.333	0.549
	1000	0.284	0.131	0.457	0.738	1.946	0.393	0.350	0.261	0.240	0.253
2	500	0.648	0.719	0.792	1.416	1.407	0.850	0.887	1.169	0.875	1.469
	1000	0.519	0.448	0.658	1.313	0.975	0.404	0.857	1.054	0.849	1.220
3	500	0.890	0.518	1.025	1.058	2.257	1.533	0.996	0.656	1.065	0.983
	1000	0.719	0.315	0.807	0.831	1.852	1.026	0.984	0.578	1.014	0.705
4	500	0.565	0.546	0.659	1.477	2.568	1.831	0.519	0.651	0.469	0.791
	1000	0.401	0.281	0.571	1.390	2.150	0.793	0.443	0.518	0.325	0.387
5	500	0.440	1.430	0.661	2.960	1.631	0.979	0.535	1.555	0.440	1.949
	1000	0.368	0.954	0.617	2.720	1.459	0.395	0.519	1.380	0.415	1.420
6	500	0.653	1.638	0.837	2.834	1.526	3.597	0.807	2.029	0.775	2.583
	1000	0.568	1.130	0.752	2.557	1.237	2.545	0.798	1.864	0.758	2.117

* Note: “Proposed method” denotes the proposed deep regression approach, “Deep PH ” refers to the deep learning approach for the partially linear PH model (Du et al., 2024), “Spline-Trans” refers to the sieve MLE approach for the partially linear additive transformation model (Yuan et al., 2024), “Penalized PH” refers to penalized MLE method for the PH model with linear covariate effects (Zhao et al., 2020), “NPMLE-Trans” refers to the nonparametric MLE method for the transformation model with linear covariate effects (Zeng et al., 2016).

cognitive function, whereas higher MMSE represents a better cognitive condition. Memory performance is mainly measured through four scores from the RAVLT, with higher values of RAVLT.i, RAVLT.l, RAVLT.d, and DelayRec indicating better performance in immediate recall, learning ability, 30-minute delayed recall, and 30-minute delayed recognition, respectively. Higher values for TrailA and TrailB reflect longer processing times to complete tasks in Test Part A and Part B, respectively, suggesting poorer executive function. The continuous variables were all normalized to have a mean of 0 and a variance of 1.

To measure the prediction performance of the proposed method, we utilized an integrated Brier score (IBS) (Tsouprou et al., 2015) calculated on the test data. Specifically, IBS is defined as

$$\text{IBS}(\hat{S}) = \frac{1}{n} \sum_{i=1}^n \frac{1}{\tilde{\tau}} \int_0^{\tilde{\tau}} \{I(T_i > t | \mathbf{X}_i, \mathbf{W}_i) - \hat{S}(t | \mathbf{X}_i, \mathbf{W}_i)\}^2 dt,$$

where $\tilde{\tau}$ represents the maximum finite value of all observed $\{L_i, R_i; i = 1, \dots, n\}$, and $\hat{S}(t | \mathbf{X}_i, \mathbf{W}_i) = \exp(-G[\hat{\Lambda}(t) \exp\{\hat{\beta}^\top \mathbf{X}_i + \hat{\phi}(\mathbf{W}_i)\}])$. Since $T_i \in [L_i, R_i]$ for each $i = 1, \dots, n$, we clearly have $I(T_i > t | \mathbf{X}_i, \mathbf{W}_i) = 0$ when $t > R_i$ and $I(T_i > t | \mathbf{X}_i, \mathbf{W}_i) = 1$ if $t \leq L_i$. When $L_i < t \leq R_i$, the exact value of $I(T_i > t | \mathbf{X}_i, \mathbf{W}_i)$ is unknown, and we can approximate it with $\hat{I}(T_i > t | \mathbf{X}_i, \mathbf{W}_i) = \{\hat{S}(t | \mathbf{X}_i, \mathbf{W}_i) - \hat{S}(R_i | \mathbf{X}_i, \mathbf{W}_i)\} / \{\hat{S}(L_i | \mathbf{X}_i, \mathbf{W}_i) - \hat{S}(R_i | \mathbf{X}_i, \mathbf{W}_i)\}$. For the special case of $L_i < t \leq R_i = \infty$, $\hat{I}(T_i > t | \mathbf{X}_i, \mathbf{W}_i)$ equals $\hat{S}(t | \mathbf{X}_i, \mathbf{W}_i) / \hat{S}(L_i | \mathbf{X}_i, \mathbf{W}_i)$. A smaller value of IBS corresponds to a better prediction performance.

To investigate the prediction performance of the proposed deep method, we conducted a 5-fold cross-validation, where the IBS was calculated with 20% of the data in each fold, and the remaining 80% of the data were treated as the training data used to estimate the model parameters. Figure S1 presents the obtained IBS values across all folds under the proposed deep regression method with the optimal model ($r = 2.6$) and the comparative methods. It shows that the proposed method leads to the smallest IBS value except for

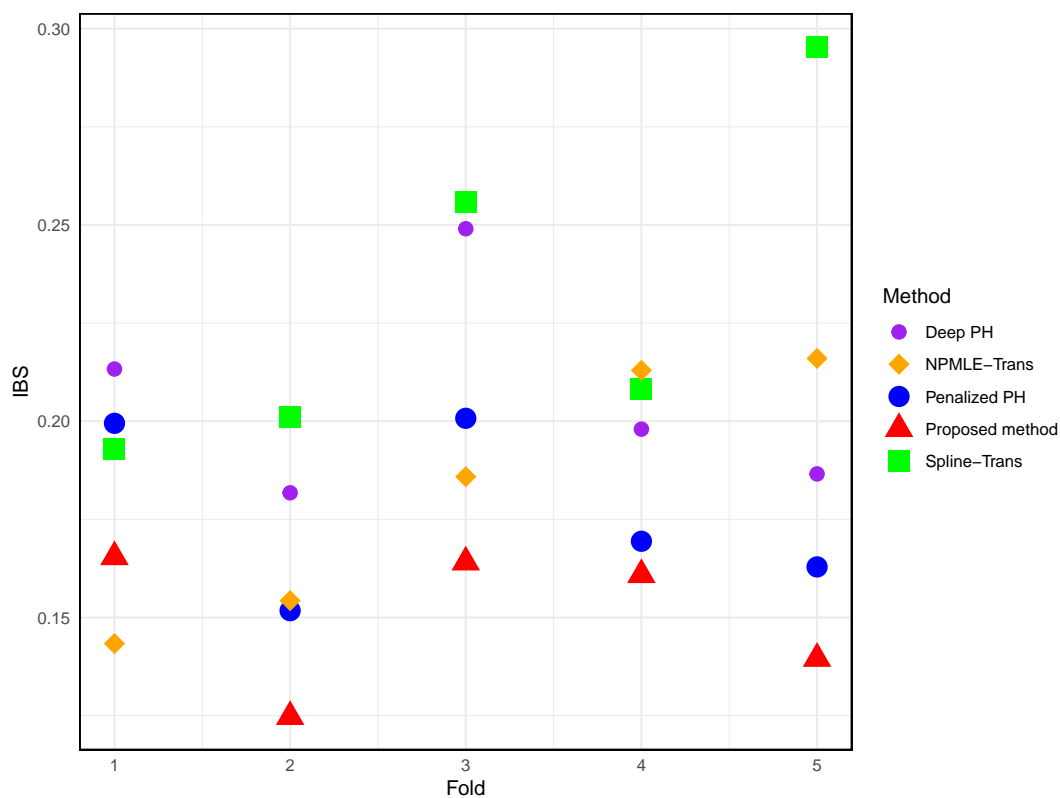


Figure S1: IBS values obtained from the ADNI data analysis.

the first fold, confirming our method’s powerful prediction ability.

References

- Bickel, P.J., Klaassen, C.A.J., Ritov, Y., Wellner, J.A. (1993). *Efficient and Adaptive Estimation for Semiparametric Models*. New York, NY: Springer.
- Du, M., Wu, Q., Tong, X., Zhao, X.(2024). Deep learning for regression analysis of interval-censored data. *Electronic Journal of Statistics* **18**(2),4292–4321.
- Goodfellow, I., Bengio, Y., Courville, A. (2016). *Deep learning*. MIT press.
- Huang, J., Rossini, A.J. (1997). Sieve estimation for the proportional-odds failure-time regression model with interval censoring. *Journal of the American Statistical Association* **92**(439), 960–967.

- Kosorok, M.R. (2008). *Introduction to empirical processes and semiparametric inference*. New York, NY: Springer.
- Lu, M., Zhang, Y., Huang, J. (2007). Estimation of the Mean Function with Panel Count Data Using Monotone Polynomial Splines. *Biometrika* **94**(3), 705–718.
- Schmidt-Hieber, J. (2020). Nonparametric regression using deep neural networks with ReLU activation function. *The Annals of Statistics* **48**(4), 1875 – 1897.
- Schumaker, L. (2007). *Spline Functions: Basic Theory*. Cambridge: Cambridge University Press.
- Shen, X., Wong, W.H. (1994). Convergence rate of sieve estimates. *The Annals of Statistics* **22**(2), 580–615.
- Tsouprou, S., Putter, H., Fiocco, M. (2015). *Measures of discrimination and predictive accuracy for interval censored survival data*. Master Thesis, Leiden University.
- Van de Geer, S. (2000). *Applications of empirical process theory*. Cambridge: Cambridge University Press.
- van der Vaart, A.W. (2000). *Asymptotic Statistics*. Cambridge: Cambridge University Press.
- van der Vaart, A.W., Wellner, J.A. (1996). *Weak Convergence and Empirical Processes: with Applications to Statistics*. New York, NY: Springer.
- Yuan, C., Zhao, S., Li, S., Song, X. (2024). Sieve Maximum Likelihood Estimation of Partially Linear Transformation Models With Interval-Censored Data. *Statistics in Medicine* **43**(30), 5765 – 5776.
- Zeng, D., Mao, L., Lin, D. (2016). Maximum likelihood estimation for semiparametric transformation models with interval-censored data. *Biometrika* **103**(2), 253–271.

Zhao, H., Wu, Q., Li, G., Sun, J. (2020). Simultaneous estimation and variable selection for interval-censored data with broken adaptive ridge regression. *Journal of the American Statistical Association* **115**(529), 204-216.

Zhong, Q., Mueller, J., Wang, J.L. (2022). Deep learning for the partially linear Cox model. *The Annals of Statistics* **50**(3), 1348–1375.